HISTOMORPHOMETRIC ANALYSIS OF BIOLOGICAL SYSTEMS

By

PRIYANKA GADAM RAO

Master of Science in Bio-Medical Engineering

University of Central Oklahoma

Edmond, Oklahoma,

2020

MASTERS THESIS

Submitted to the Faculty of the
Graduate College of the
University of Central Oklahoma
in partial fulfillment of
the requirements for the Degree of
MASTER OF SCIENCE
MAY 2020

HISTOMORPHOMETRIC ANALYSIS OF BIOLOGICAL SYSTEMS

Thesis Approved:

Committee Chair: Dr. Morshed Khandaker

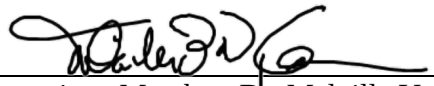

Committee Member: Dr. Melville Vaughan

Committee Member: Dr. Scott Mattison

ACKNOWLEDGMENTS

I would like to express my gratitude to Dr. Morshed Khandaker for allowing me the opportunity to do my research thesis with him and for his help, support and understanding throughout my master study and research. His direction and advice helped me at all times, and I could not be more thankful. I would also like to thank Dr.Melville Vaughan and Dr.Scott Mattison for their encouragement, suggestions and taking out time to participate in my thesis research.

I would also like to appreciate the Department of Engineering and Physics, the College of Mathematics and Science, and Graduate college at University of Central Oklahoma. I am grateful to all the professors at the department of engineering and physics involving Dr. Gang Xu and Dr. Mohamed Binjabr for their suggestions and encouraging words during my independent study. I would like to thank my research mate, Shawn Whittaker for his constant support, partnership and guidance. Also, I am filled with gratitude for I am very happy that UCO accepted me as a master's student.

Finally, I would like to thank my parents and sister, deep from my heart for allowing me to be the person I am and pursuing my masters. I would also like to thank my uncle, Balaji, for the constant support and encouragement.

HISTOMORPHOMETRIC ANALYSIS OF BIOLOGICAL SYSTEMS

Priyanka Gadam Rao

May 2020

ABSTRACT

Histomorphometric analysis is the histologic sectioning of normal and diseased samples. Over previous decades, certain techniques and analysis have not been recognized in a long time causing them to lack in solutions that they are looking for. In this study, we have applied a histomorphometric analysis technique for three different biological systems. These systems include skin, cartilage and bone tissue. Skin constitutes its tissue in the epidermis, cartilage represents tissue engineered intervertebral discs and titanium interfaces with bone cement.

The first part of the study quantified the biological functions of the epidermis, dermis anchored with an in vivo study of the graft model with electro spun nanofibers using Bartlett's test, Image J and one-way ANOVA test.

The second part of the study involved a developed graft model that mimic the structure and function of the dermis by using Electrospun Nano fiber coating to depict collagen, polyethylene Glycol Diacrylate(PEGDA) and poly e-caprolactone (PCL) scaffolds which were cultured using rat dermal fibroblast cells and quantified by finding comparisons and region of interest (ROI).

The third part of the study concentrated on electro spun nanofiber coating techniques used to design Polyethylene Glycol Di-acrylate (PEGDA) tissue engineering scaffold for bone substitute. Mechanical and biological functions of titanium implant were successfully improved and were compared accordingly using Bone J and MATLAB.

The outcome of the study has been successful and for future research, quantification may help further evaluate tissue grafts, implants and find more parameters within a tissue.

TABLE OF CONTENTS

LIST OF FIGURES

LIST OF TABLES

LIST OF ABBREVIATION

RDF: Rat Dermal Fibroblasts

PCL: Polycaprolactone

CG: Collagen

PEGDA: Polyethylene Glycol Diacrylate

PBS: Phosphate Buffer Solution

Ti: Titanium

NF: Nanofiber

ENF: Electrospun Nanofiber

HMA: Histomorphometric analysis

NP: Nucleus Pulposus

AF: Annulus Fibrosis

H&E: Hematoxylin Eosin

PR: Picrosirius Red

PMMA : Polymethyl methacrylate

BIC: Bone to Implant Contact

Chapter 1

1. INTRODUCTION

1.1 HISTOMORPHOMETRIC ANALYSIS

1.1.1 Introduction

Image processing is a technique that is used to perform operations on an image, in order to receive an enhanced image or to extract useful information from it. [1] Histomorphometry is defined as the measurement of the shape or form of a tissue. Using image processing, quantitative analysis of an architecture is achieved with this technique which provides valuable information. It will determine measurement of the analysis based on shape, size and volume of a tissue. It consists of various valuable parameters consisting of a range from its area to migration of cells from one place to another.[2] Quantitative analysis of bone architecture is achieved in the *in-vivo* study of titanium implants by using bone histomorphometry which provides valuable information on the amount of bone and its cellular activity.[3] To perform histomorphometric analysis, instrumentation of softwares is key and ability to measure performance, detect abnormalities and compare results by understanding its development. [4, 5] With such monitoring, by finding the right tools and softwares, this will help gain insight by measuring and understanding the processes accordingly.

1.1.2 Methods/Software package used in Histomorphometry analysis

1.1.2.1 Image J

This program is an analysis program using to observe and measure biological factors and beyond. It contributes to various factors present in an image such as supporting image data, permitting new collaborations, maintain compatibility with certain functions and broaden its use not just to one material but to several other materials as well. [6, 7]It has a wide range of software

tools present and include phenomenal platforms such as MATLAB and R programming. This software supports various formats and image stacks, a sequence of images that combine to form a single window.[8] Also, it supports geometric transformations, density histograms, scale measurements, conversions and contrast manipulation.

1.1.2.2 Bartlett's test

This test conducts variances that are equal to several other samples. Thus, it is usually done by calculating its assumptions before running its absolute statistical tests which originates from a normal distribution. Here, equal variances are called homoscedasticity and helps construct alternative hypothesis as well. According to its test procedure, it is based on its statistics where distribution of samples providing an approximate value chi-square distribution with certain degrees of freedom called (k-1) where k is equal to the number of samples, changing in size and is derived from independent normal distributions. It is a sensitive test and is used to sample normality and non-normality.

1.1.2.3 ANOVA test

ANOVA test is a certain visual in observing if its results are significant to quantify. So, it helps reject values and determine if there is a difference between them. This test consists of two groups : one-way and two-way. [9] Here, one-way ANOVA test is used and has one independent variable where two groups are involved, and it can quantify the difference and value between them. Using F-distribution, this certain technique can only be used for numerical data and one-variable data stating samples derived from its mean values. [10]Thus, by testing null hypothesis, its necessary to know that this respective test cannot specify which group is significant from the other.

1.1.2.4 Bone J

This software program is a collection of biological plug-ins related to the bone tissue images. It is a certain plug-in from Image J which complies with its modern architecture containing support in its hyper stacks respectively. [11] According to its development, it helps provide measurements in its geometry followed by its standard bone measurements within an image such as thickness, connectivity, scale measurements, conversions and density.[12] They are known to be called

Image J macros as it helps understand the sequence of menu commands along with its active development.

1.1.2.5 MATLAB

MATLAB is a software program that combines analysis and design with a program language leading to creating scripts with a summation of its code, output, implementation of functions, algorithms and error detections. [13]In this image analysis, it helps provide measurement in various aspects of an image such as area, density, perimeter, thickness and intensity followed by creating a certain validation to other software programs. Therefore, the set of tools and programs facilitates management of data and variables for applying complex variances and values in order to solve and quantify analysis simultaneously. [14, 15]

1.1.3 Limitations in currently used methods

Drawbacks may deal with differences in staining techniques, methods to measure the specimen and time being a factor. Staining techniques can overcome its variation by converting is images without color to make it even enough to analyze. Each method has its own technique however validation is necessary to make sure each technique used is adjacent to its other measurements respectively. One of the main factors that cause the measurements to lack is its time. Therefore, to overcome time, it can be done by common techniques that makes it quite simpler to analyze.

1.2 TISSUE ENGINEERED BIOLOGICAL SYSTEM:

1.2.1 Introduction

Tissue engineering basically refers to merging respective fields such as cells, engineering, materials as well as biochemical factors to replace or improve biological tissues. [16]According to Figure (1-1), It is the field of development in biomaterials which involves incorporating scaffolds, cells and biologically active molecules into functional tissues. This principle helps in determining how the cells respond to signals, interact with the environment and help to restore damaged tissues. Therefore, once cells are thawed, it undergoes cell culture followed by harvesting them for about 28 days. It involves the use of a tissue formation of new viable tissue for a medical purpose.[17]

Also, tissue engineering has known to help on one focus that this field has taken is the understanding of tissue and organ development during embryogenesis, as this knowledge will open avenues to new applications of this technology. [18, 19]This field integrates collagen, polyethylene glycol and polycaprolactone by providing aid in replacement of damaged rat dermal fibroblasts (animal model) respectively. [20]

1.2.2 Intervertebral disc graft

This is a part of the body that is composed of a network of collagen fibers and gelatinous material that helps provide tensile strength creating flexibility and durability.[21] This material is far better than bone as it helps holding bones together and supports other tissues as well. The intervertebral disc comprises of the annulus fibrosis and nucleus fibrosis. According to the nucleus pulposus, it is a soft region with filling present at the center of the intervertebral disc. Its function is compressing pressure by distributing it throughout the disc.[22] With pressure being transported, this avoids concentration in stress as it might lead to injury or damage to the endplates of the disc. Its structure as shown in Figure (1-2), it contains loose-like fibers that are unseen in the mucoprotein gel. Not only does it help with pressure, it is known to be a shock absorber. This absorbs body's activities by not trying to create any ruckus between the two vertebrae. Another part of the intervertebral disc is the annulus fibrosis seen in figure (1-2). It is located as an outercoat of the intervertebral disc. It is defined as short and comprises of several concentric shaped rings of fibrous cartilage. Its function is to increase the strength as a whole part of the disc.[23]

1.2.3 Bone graft

Bone is a certain body tissue containing collagen and calcium phosphate making up various bones of the system in the body.[24, 25] It helps provide structural support and environment for where blood cells are produced. Since they have their own blood vessels, this material can help them grow and repair themselves. It comprises of a hard-outer layer and a spongy inner layer. The hard-outer layer is known as cortical bone providing strength and density properties. Also, a spongy inner layer is called a trabecular bone which is lighter, and density is lesser than its cortical bone. Grafting procedure takes place by being beneficial enough to fix them as they are replaced by injuries or trauma respectively. It usually is obtained from a donor or body which may be entirely synthetic creating a network of different types of graft. [26]Thus, grafting is done using

titanium implants and PMMA cement surface to measure its compatibility and contact within each other.[27]

1.2.4 Skin graft

Skin is known to be the tough, outer protective layer of the body's surface that provides shielding and obtains sensory stimuli from external surroundings. The skin comprises of the epidermis, dermis and subcutis. Epidermis is the protective part of the layer providing a protective structure. Dermis consists of a fibrous layer supporting and strengthening it outer part of the layer (i.e.) epidermis while subcutis consists of fat underneath the dermis respectively. [28, 29]Grafting is a certain process that involves removing skin from one area of the body and transferring it to another area of the body. Surgery is usually done for this type of grafting and consists of two types: split thickness and full thickness graft. Therefore, grafting is done by producing skin through cell culture comprising of collagen and PCL nanofibers, replacing it with normal skin of a rat.[30]

1.3 ELECTROSPUN NANOFIBER BASED 3D TISSUE GRAFTS

1.3.1 Electro spun Nanofiber

Electrospinning is a certain technique used to spin to produce nanofibers respectively. Producing nanofibers by the electrospinning process has been increasingly trending because of it being effective enough to make extremely fine fibers with diameter in the range from several micrometers to several nanometers. [31, 32]The main components of this process are a high voltage supplier, pump injector, collector, small diameter tube, syringe, and a needle. Various electrostatic polymer and solvent for dissolving polymer are used to produce the nanofiber. [33]

1.3.2 Poly-ε-caprolactone (PCL)

Due to its low cost, biocompatibility, and slow bio resorption, poly-ε-caprolactone (PCL) is used as a polymer to produce the nanofiber for various applications. PCL is a versatile polymer and is used in various long-term biodegradation biomaterials.[34] A lo degradation of 3-4 years makes PCL more suitable for long-term degrading implants and applications. The distinct

rheological and viscoelastic properties of PCL and the ease to produce nanofibers makes PCL as a widely used biomaterial. It is also used in drug delivery devices which are approved by Food and Drug Administration (FDA).[35]

1.3.3 Tissue engineering application of PCL

PCL is used is to enhance in vitro and in vivo biocompatibility properties of PEGDA scaffold by coating it with PCL nanofiber matrix for its application in intervertebral disc (IVD).[36] Skin uses collagen and PCL to develop a dermal equivalent scaffold to generate normal skin performance. PCL electro spun nanofiber assembles with collagen and helps develop dermal equivalent scaffold.[37] To cure bone defect due to disease, metal (e.g. titanium) implants and bone cement (PMMA) are used. PMMA cement o hold the implant in place. PCL fiber can be coated on metal implant and PMMA to improve their biological factors. [38]

1.4 MATERIALS USED FOR IVD GRAFT

1.4.1 PEGDA

Polyethylene Glycol Di-acrylate (PEGDA) is manufactured easily to permit cell growth at higher depth using a process called photolithography. Photolithography is a process which is commonly used in microfabrication to produce the desired scaffolds with a high level of detail and precision. It is a 3D network structure. It is used for allowing the constructions of channels within the scaffold to better distribute nutrients to the cells. PEGDA tissue scaffolds have thickness higher than 1 mm and were shown to have limited applications as a three-dimensional (3D) cell culture device due to the inability of cells to survive within the scaffolds. Without permission to adequate nutrients, cells placed within the PEGDA tissue construct having thickness higher than 1 mm fall out, leading to tissue regeneration to be non-uniform. One of the goals of this thesis is to determine its regional properties as well as its migration and presence of scaffolds in the implants respectively.

1.4.2 PCL

(PCL) is one of the earliest, commercially available, synthetic polymers distinguished by a large set of biodegradation and mechanical properties that can be finely ruled by regulating the local environmental driving forces (i.e., microorganisms, enzymes, hydrolysis). Owing to their faster resorbability and long-term degradation in the presence of water (up to 3 to 4 years), PCL has been widely detected as a material able to target selective cell response. It is a biodegradable polyester with a low melting point of around 60 °C and a glass transition temperature of about −60 °C.[32, 33] The most common use of polycaprolactone is in the production of specialty polyurethanes. Polycaprolactones impart good resistance to water, oil, solvent and chlorine to the polyurethane produced.

Polycaprolactone (PCL) has been widely used in long-term implants and controlled drug release applications. However, when it comes to tissue engineering, PCL suffers from some shortcomings such as slow degradation rate, poor mechanical properties, and low cell adhesion. [39]The incorporation of calcium phosphate-based ceramics and bioactive glasses into PCL has yielded a class of hybrid biomaterials with remarkably improved mechanical properties, controllable degradation rates, and enhanced bioactivity that are suitable for bone tissue engineering.[40]

1.5 MATERIALS USED FOR BONE DEFECT REPAIR

1.5.1 PMMA

Bone cement is used in various orthopedic surgeries. Among the many potential bone cement materials, polymethylmethacrylate (PMMA) bone cement has been successfully used in orthopedic surgeries mostly because of its strong mechanical bonding with implant. PMMA bone cements are provided as two-component materials, a powder (PMMA beads) and a liquid (MMA monomer). These two components are mixed at 2:1 ratio and polymerization occur. [27, 38]The current most commercially available PMMA bone cements are Cobalt (Biomet, Inc.), Simplex (Stryker, Inc.), and Palacos (Heraeus Company), and Veterinary bone cement (Bio Medtrix, LLC).

However, several drawbacks associated with PMMA bone cement limit its efficacy. For example, PMMA cement adheres inadequately to the bone surfaces (no bioactivity) , has a high exothermic reaction temperature and exhibits monomer toxicity. Particularly, enough bonding strength of cement with the implant and bone is required for the design of optimal bone cement. Whereas, increasing the bonding strength of implant-cement interfaces is imperative. It may be accomplished by increasing the surface interlock of implant-cement or bone-cement interfaces through enlarging the surface roughness of the cement mantle or the implant surface.

1.5.2 Titanium

Titanium alloys are metals that are a mix of titanium and other chemical elements. Their properties are that they have very high tensile strength and toughness. [41]They are also light in weight, have corrosion resistance and the ability to withstand extreme temperatures.

Titanium based alloy have been mostly used in orthopedic and dental surgeries as implants because of their strong mechanical, chemical, and biological properties. The conclusion of Ti into the body is very concerning because Ti metal surface can instantly form a stable and inert layer of titanium dioxide (TiO_2), which will prevent Ti metal from reacting with body fluid.[42] Ti has its excellent biocompatibility such as high corrosion resistance and low level of electronic conductivity. Comparing to commercial pure Ti and among the various Ti alloys, Ti-6Al-4V, which was used in this in-vivo study, is the most widely used as implant because of its better physical and mechanical properties in comparison to pure Ti.

1.6 MATERIALS USED FOR SKIN GRAFT

1.6.1 Collagen

Collagen is known to be the most abundant protein in human body. It consists scaffolds to provide strength structure, especially for skin, bones, and connective tissues.[43] Collagen is an important building block for the skin. The principal protein of the skin, tendons, Intervertebral disc , bone, and connective tissue. Collagen is an essential part of the framework of the design of our

various body tissues. It makes up to 30% of the protein in our body and 70% of the protein within our skin. Collagen helps our skin stay toned and supple. The dermis, which provides the foundation for the skin, is closely involved in the skin's elasticity and flexibility, and the main source of collagen in the skin. [44]In this skin, staining of the scaffold helps differentiate collagen accordingly as it helps to provide an effective way in characterizing and analyzing new information during regeneration. In this title, there are two types of collagen: Endogenous and Exogenous collagen.

Endogenous collagen is natural collagen, synthesized by the body. Exogenous collagen is synthetic. It comes from an outside source, such as supplements. Endogenous collagen has a number of important functions. Breakdown and depletion are linked to several health problems. Exogenous collagen is used for medical and cosmetic purposes, including the repair of body tissues.

1.7 MOTIVATION AND GOALS

The motivation of this research thesis was to evaluate each tissue comprising of skin, Intervertebral disc and bone using softwares that help each graft and implant. The goal is to develop an image processing technique for all three tissues and make sure the invitro studies of the skin and Intervertebral disc are being produced in a timely manner.

1.8 OBJECTIVE

The objectives of this thesis are: 1) Developing a skin equivalent base using RDF cells and image processing using histomorphometric analysis, 2) Producing Intervertebral disc and it's in vivo process using image processing consisting of histomorphometric analysis, 3) In vivo analysis of titanium implant architecture is achieved by using bone histomorphometry which provides valuable information on the amount of bone and its cellular activity.

1.9 ORGANIZATION OF THESIS

Figure 1-3 depicts the schematic flowchart of the thesis study outline. This thesis contains 8 chapters. Chapter 1 is the introduction of the research thesis. Chapter 2 involves the in-vitro and in-vivo methods of sectioning and histomorphometric analysis of the Intervertebral disc Chapter 3 includes the in-vivo study of histomorphometric analysis of the titanium implants of the bone. Chapter 4 demonstrates the in-vitro and in-vivo study of equivalence and histomorphometric analysis of the skin. Chapter 5 draws in the limitations of image processing. Chapter 6 necessitates the future work and plans for this thesis. Chapter 7 entails the conclusion of the thesis.

1.10 FIGURES

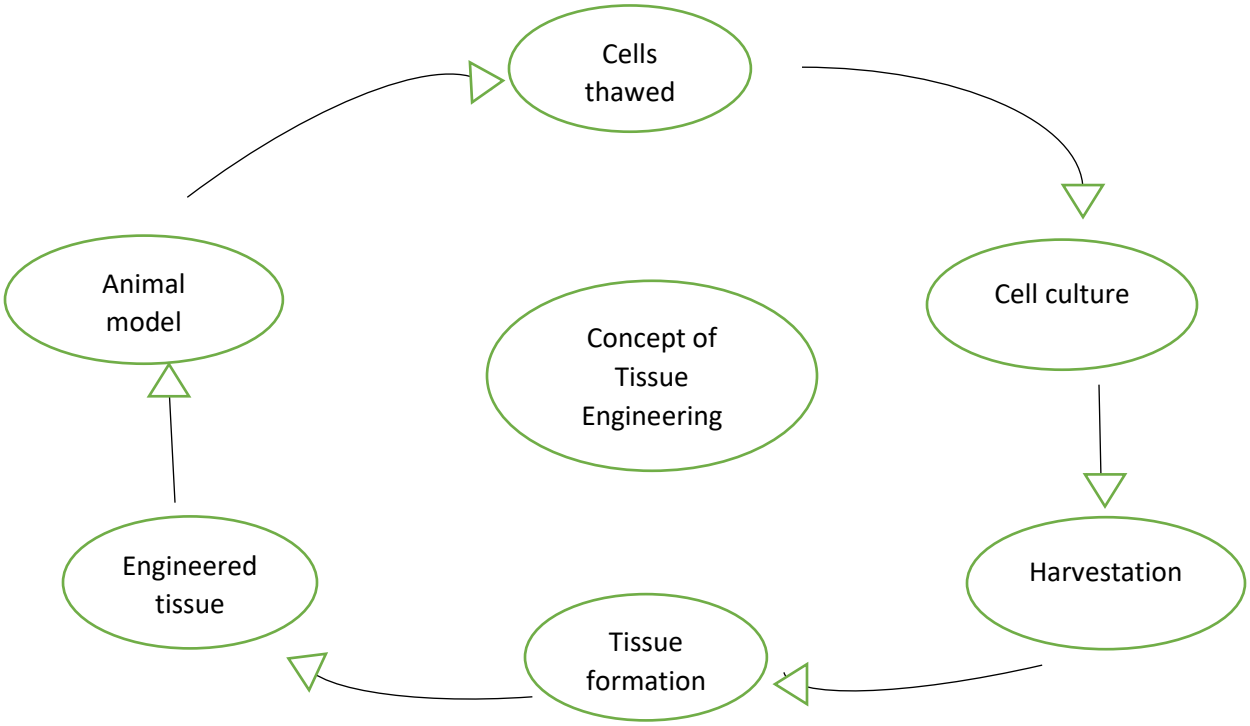

Figure 1-1 Flow diagram of the biological system in tissue engineering

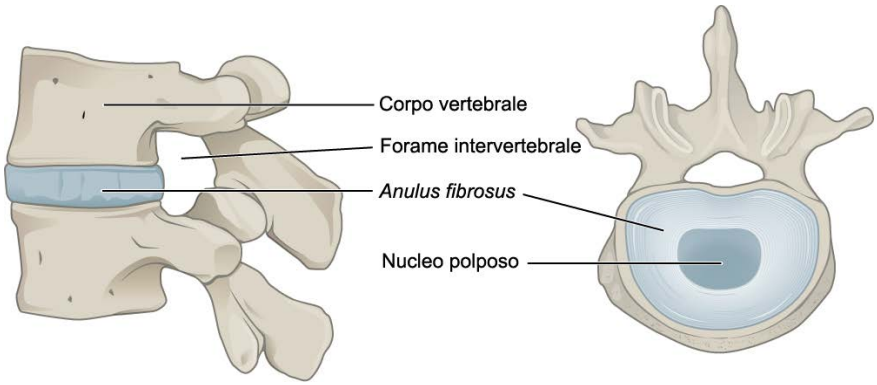

Figure 1-2 Annulus fibrosis and Nucleus pulposus in an Invertebrate disc

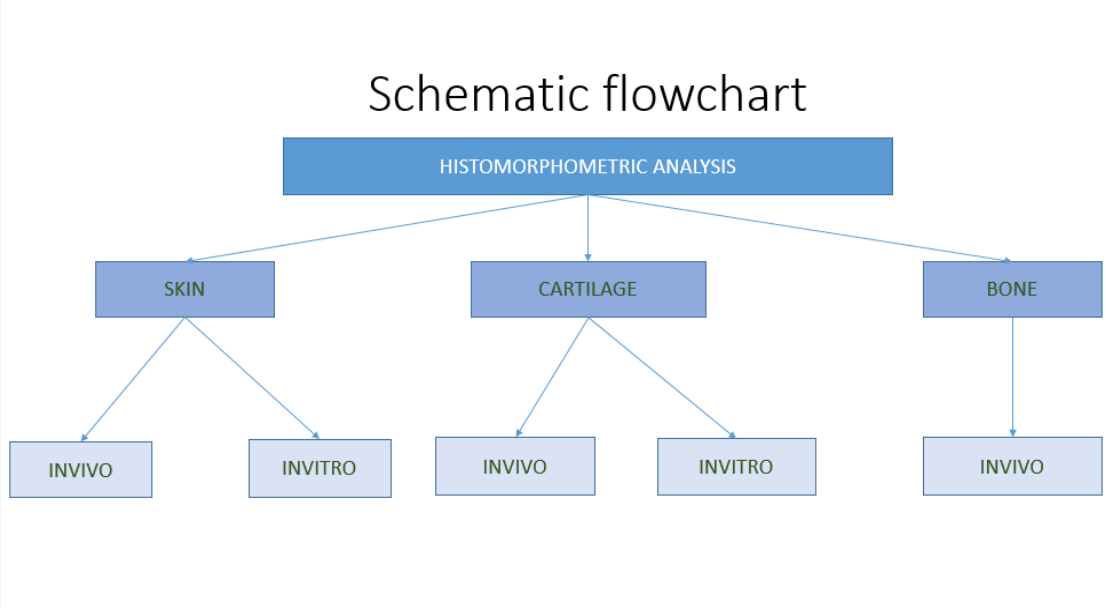

Figure 1-3 Schematic flowchart of the thesis study outline

Chapter 2

EFFECT OF POLYCAPROLACTON NANOFIBER COATING ON POLYETHYLENE GLYCOL DIACRYLATE SCAFFOLDS FOR TISSUE REGENERATION: AN *INVITRO* AND *INVIVO* STUDIES

2.1 SUMMARY

The goal of this study was to enhance the in vitro and in vivo biocompatibility properties of a polyethylene glycol diacrylate (PEGDA) scaffold by coating it with polycaprolactone (PCL) nanofiber matrix (NFM) for its application in cartilage and/or intervertebral disc repair. This study examined two groups of scaffolds, PEGDA, and PEGDA coated with PCL, referred to as PCL-PEGDA. In vivo results confirm that PCL coated PEGDA scaffold was able to maintain IVD space and created proteoglycan and collagen-rich matrices after 4 weeks of scaffold implantation in caudal disc space. Therefore, the developed PCL-PEGDA has the potential to be tissue-engineered into intervertebral discs or cartilage implants. Therefore, biocompatibility of tissues is observed over time. Histomorphometric analysis is done by analyzing its quantifying its cells respectively. It helps compare the values of each tissue followed by its outcome from its simultaneous invitro analysis.

2.2 INTRODUCTION

A hydrogel is an essential class of hydrophilic polymer with applications in tissue engineering. Several researchers studied polymeric hydrogels, such as silicones, polyurethanes , polyethylene, polyvinyl alcohol, and polymers reinforced with fibers or ceramics as an implant material for Nucleus pulposus (NP). Even though these polymers exhibit similar characteristics like the natural intervertebral disc (IVD) in terms of biomechanical behavior, they are considered inappropriate materials for IVD restoration due to their inadequate stiffness and poor cellular responses between the implant and biological environment.[21, 45] Thick hydrogel scaffolds have limited physical

(porosity, hydrophobicity), mechanical (stiffness, elasticity) , and biological (cell growth and differentiation of cells) properties. For example, cells were unable to survive polyethylene glycol diacrylate alginate (PEGDA) scaffolds having a thickness higher than 1 mm without a porous network. There is a significant need for research to investigate methods that can overcome the limitations exhibited by thick hydrogel scaffolds for intervertebral disc and cartilage repair.[46]

2.3 MATERIALS AND METHOD

2.3.1 Materials

This study involves materials such as Phosphate Buffer Solution (PBS), 5 % harvest media, Trypsin dye solution, PCL pellets and acetone, an active reagent used in electrospinning of nanofibers. Once placed in a sonicator machine for 30 minutes, it is immediately poured into a syringe and attached to a 9 kV power supply creating fibers on a two-pole wood stand creating PCL fibers. PEGDA is obtained by producing a photo initiator mixture combining a photo initiator of 0.3 grams and 1 ml of vinyl-2-pyrolidinone.[28, 32] This is blended with PBS solution and photo initiator mixture of 0.4 microliters is produced by associating the newly made PEGDA placed in a mold of silicone creating a scaffold with a diameter of 10 mm and thickness of 0.94 mm.

A 3D cartilage graft was produced through cell culture using Rat dermal fibroblast cells with Collagen, PEGDA and PCL due to its stable biocompatibility and mechanical properties within the respective field under standard cell culture condition. Meanwhile, electro spun nanofibers were obtained using a sonicating machine to receive PCL-PEGDA scaffolds.[33, 47, 48] Later, the samples were placed in a 48-well plate distributed into each well equally. This Olympus fluorescent microscope (Bx41) is a certain imaging technique that uses reflected light and sample fluorescence to capture images within the cell tissue. However, the potential application of PCL NFM coated PEGDA in IVD, or cartilage repair requires further in vitro biocompatibility studies using bone generating cells and in vivo biocompatibility studies using an appropriate animal model. Histomorphometric analysis is calculated followed by its Nucleus Pulposus (NP) area, Annulus Fibrosis (AF) area, mean, cell density and respective content from stained images. Quantitative measurements of stained images such as New cell matrix (H&E stain), Collagen

(Picrosirius red stain) and Proteoglycan (Alcian blue stain) are calculated to display comparisons in their content values respectively. Each parameter is obtained by calculating and showing differences in each stained image after 28 days in the respective disc space. This presents quantitative value of each property. [49-51]

2.3.2 Preparation of samples

Cartilage is used to obtain a structure and function of an interactive local cartilage tissue combined with the following tissue cells, three-dimensional scaffolds, and extraneous parameters such as cell viability and biocompatibility tests.[52] Initially a graft is assembled by performing cell culture on the thawed cells and cell viability is measured accordingly. 24 hours after this procedure, the dish is washed with PBS solution to observe its cell adhesion and how much the cells were attached to the base. After 48 hours, cells were placed firmly with 4% of paraformaldehyde. After some time, the sample dish is washed thrice by PBS in an interval of 5 minutes. Trypsin and media are added and later replaced with PBS solution. Thus, these cells are visible and counted using Olympus fluorescent microscope Bx41 with a magnification of 10 x.

2.3.3. Staining methods

There are three method of staining involved in the study of cartilage (i.e.) Hematoxylin and Eosin stain (H&E), Picrosirius Red stain and Alcian Blue stain. [49, 51, 53]For H&E stain, a certain protocol is followed with a sequence of steps. These are two separate stains yet go hand-in-hand. Hemotoxylins are used in specific stains illustrating certain elastin and myelin fibers while Eosin Y is a stain that helps intensify the structures that hematoxylin tends to stain. It can be mixed with alcohol or water. The initial process of this staining is done by extracting the paraffin wax with xylene for 3 minutes and this step is done twice. Once waxing is removed, this slide is poured into 100 % ethanol twice with an interval of 2 minutes each and then, dipped into 95 % alcohol followed by rinsing with water for hydration. Hematoxylin stain is used by staining the slide completely in order to stain the nuclei for 3 minutes and completely rinsed with water. An alkaline solution is involved by washing the slide with it and so, this creates a type of blue color within it followed by

a rinse with water. Then, it is poured into 95 % ethanol respectively to remove excess stains. Eosin stain is now used making the stain produce a pinkish color. Later, 95 % ethanol helps clean the unnecessary stains in the slide followed by 100 % ethanol twice and poured with xylene twice. Pictures are taken using the Olympus fluorescent microscope (Bx41).

The second stain known as Picrosirius Red stain follows an initial procedure by removing the paraffin wax from the sample. This slide is now stained with hematoxylin for an approximate duration of 8 minutes and followed by washing it with water twice in intervals of 5 minutes specifically for hydration. Later, it is dipped into the picrosirius red stain and remains in it for about an hour to provide near-equilibrium area.[49] Once this is done, the slide is rinsed with alkaline solution to remove any excess stains from the slide respectively and is rinsed with water. 100 % ethanol is used three times to clean the slide followed by dipping it into xylene.

Alcian Blue stain, the third and last stain is used for proteoglycan. This process is followed by removing the paraffin wax from the sample and rinsing the slide with water for respective hydration. This is later stained in alcian blue stain for a duration of 30 minutes and then, the slide is rinsed with water twice to remove any unnecessary stains from it. It is dipped into fast red stain which is a combination of 0.1 grams of Nuclear fast red dye and 5 grams of aluminum sulphate. This is kept for about 5 minutes followed by rinsing with water and going through 95 % ethanol twice with intervals of 3 minutes each. Finally, it is cleaned with xylene. [51]

2.3.4 Histomorphometric analysis

The rat tails were preserved in 10% phosphate-buffered formalin and were fixed at room temperature. Specimens were embedded within the acrylic resin, and serial sections of 0.5 mm were cut using a rotatory manual microtome.[4] Each section was stained with hematoxylin and eosin stain for new cell-matrix detection, alcian blue for proteoglycan detection, and picrosirius red staining for collagen detection. The slides were imaged by bright-field or polarized light microscopy.

Quantification is obtained by measuring its parameters involving cellular activity. It can be analyzed by various image processing softwares. According to figure, it consists of H&E stain, Picrosirius Red stain and Alcian Blue stain. Therefore, these tissues have differences in the

Nucleus Pulposus and Annulus Fibrosis respectively. According to the SHAM samples, NP gels had been extracted due to the disc space collapsing. [54, 55]PCL-PEGDA samples also had their NP gels extracted but was substituted with their PCL-PEGDA material and thus their measurements were extremely like the native image samples. This helps create comparison between the three samples.

2.4.1 Method of Analysis

The cartilage of rat tail was immersed in PBS solution at room temperature. Later, these samples are fixed firmly with acrylic resin with a cut of 0.5 mm circular microtomes followed by staining of H&E stain for new cell matrix, Picrosirius stain for collagen and Alcian Blue for proteoglycans. This study involved image processing softwares such as Image J to create a boundary of NP and AF areas in order to calculate the region of interest. A centerline is created to find the boundary of region of interest for AF. [56]X and Y length is found by creating lines of boundary of the AF area, respectively. Also, calculation of each stain and their content, areas and region of interest were determined using this software. The slides were imaged by bright-field or polarized light microscopy. Using Image J for NP and AF areas, area specific region of interest (ROI) for each slide had been calculated. After drawing the boundary of NP. A centerline is manually drawn that bisected NP area. Two parallel lines at a certain distance, t, from the centerline was used to draw the boundary of ROI for AF area. The total AF area in the ROI is the summation of two regions, which is marked by A and B. The software calculated total the NP and AF areas from each image. In addition, the software calculated the stained area of new cell matrix, proteoglycan, and collagen in the marked NP and AF areas.

2.5 RESULTS AND DISCUSSION

The study shows that the PEGDA samples were prepared, applied to the wistar rat species in Figure (2-1) and the rat was euthanized later that respective month. It was split into several parts where the sample had been surgically implanted and placed into histology causing differences between them. Therefore, native images are those that are normal and do not have any implants within

them. Sham images are pulled out and replaced with nothing inside. PCL-PEGDA is the substitute when the cartilage of the rat was taken out and replaced with this respective sample. Staining procedures were done simultaneously, and quantification began. Each image is not like the other and provides differences so therefore, analysis can be done to other images as well using this similar tool.

According to the tables below, it presents the quantitative value of the presence of new cell-matrix, collagen, and proteoglycan at NP and AF areas in native and PCL-PEGDA implanted (table 2-1(c)) samples after 4 weeks. Since there were no definite NP and AF areas in the sham group (table 2-1 (b)), it was irrelevant to compare collagen and proteoglycans contents of the sham group with the other groups. In comparison to the native IVD (table 2-1 (a)), the implanted group showed less amount of H& E, hydroxyproline, and picrosirius red content staining. H& E, collagen and proteoglycan content was seen in the AF regions for all groups, but with increased content in the native group compared to the other groups, as seen by histology analysis. Histology analysis results also show the differences in H&E, collagen, and proteoglycan content values between the implanted and native AF and NP after 4 weeks in the disc space.

2.6 CONCLUSION

According to the analyses, histomorphometry technique was able to signify each stained image and the comparison between them. Also, properties of samples during cell viability test, cell adhesion and measurement of region of interest can be concluded from the present observation:

1) Cell viability has found out to be feasible during the in vitro analysis as it was observed to be a little high and PCL-PEGDA samples were quite attached to the surface of the well plate. Thus, sample cells were able to attach well to the PEGDA scaffold.
2) Based on histomorphometric analysis results, native and PCL-PEGDA samples found to be similar in values. Since NP area is not available in the SHAM samples, NP area of collagen and proteoglycan were not found however AF areas were found in all stained images.

2.7 FIGURES

Figure 2-1 Image of a rat tail

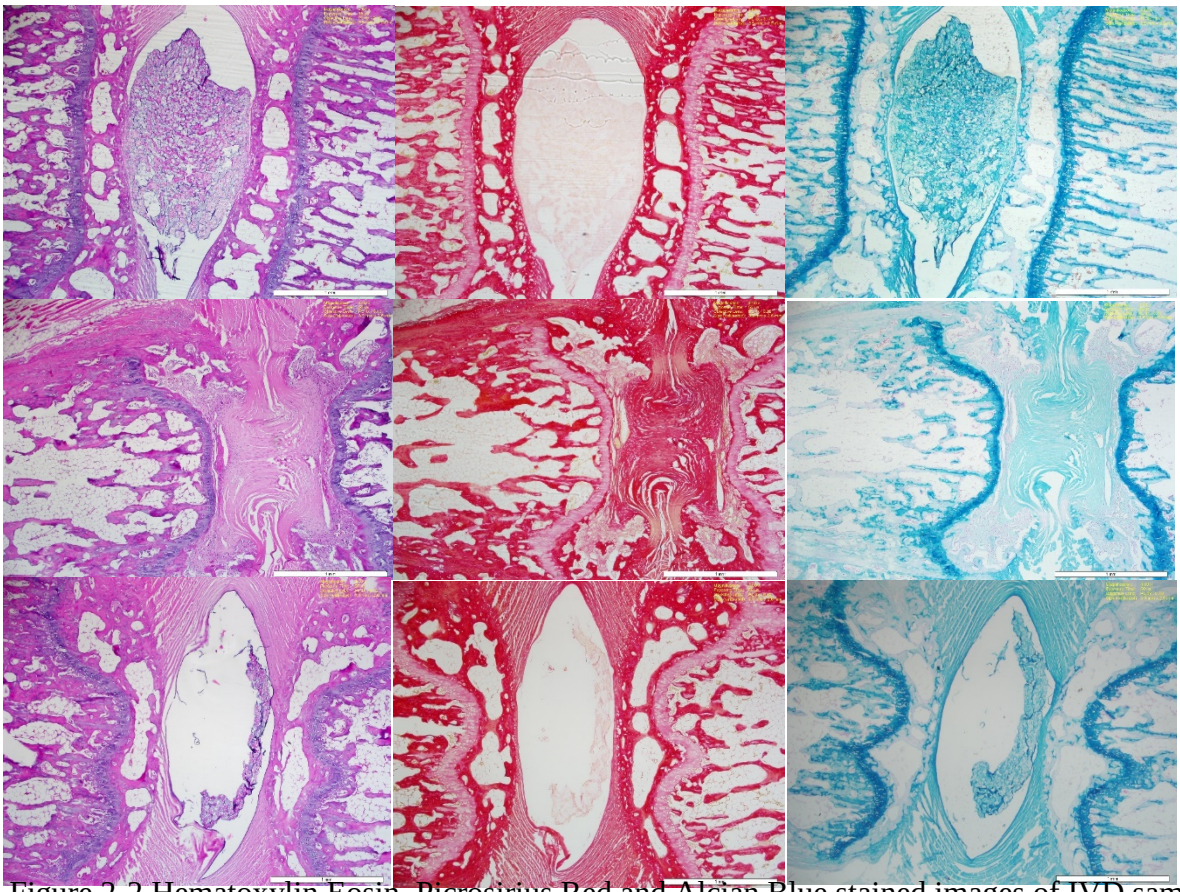

Figure 2-2 Hematoxylin Eosin, Picrosirius Red and Alcian Blue stained images of IVD samples: (a) Native samples (b) Sham samples (c) PCL-PEGDA samples

2.8 TABLES

Table 2-1 Reference values regarding histomorphometric parameters between native and PCL-PEGDA histology slide samples. The values of all parameters were reported as mean ± SD (*n*=3).[57]

Histological analysis parameters (mm^2)	**Native**	**PCL-PEGDA**
NP area	2.40±0.03	2.35±0.02
H&E stained area in NP	0.63±0.03	0.40±0.04*
Proteoglycan content in NP	0.62±0.04	0.43±0.03*
Collagen content in NP	0.64±0.03	0.41±0.04*
H&E stained area in AF area*	1.90±0.2	1.62±0.2
Proteoglycan content in AF area *	1.79±0.1	1.80±0.1
Collagen content in AF area *	1.78±0.1	1.64±0.1

Table 2-2(a). Histomorphometric analysis data for IVD native samples where values of all parameters reported as mean± SD (n=3)

HISTOLOGICAL ANALYSIS PARAMETERS	H&E STAIN (NATIVE)	PR STAIN (NATIVE)	AB STAIN (NATIVE)
X(mm)	0.032	0.035	0.036
Z(mm)	0.034	0.036	0.039
Total AF in the ROI (mm^2)	2.25	2.56	2.22
Total proteoglycan in NP (mm)	-	-	0.68±0.02
Total proteoglycan in AF (mm)	-	-	1.69±0.1
Total collagen in NP (mm)	-	0.66±0.03	-
Total collagen in AF (mm)	-	1.61±0.2	-
Total new cell matrix in NP (mm)	0.72±0.04	-	-
Total new cell matrix in AF (mm)	1.85±0.2	-	-
Area of NP (mm^2)	2.35	2.44	2.41
Mean of NP (mm^2)	$3.92x10^{-3}$	$7.88X10^{-3}$	$2.72x10^{-3}$
Density of NP (mm^2)	$0.599x10^3$	$0.309X10^3$	$0.886x10^3$
Area of AF (mm^2)	2.61	2.68	2.6
Mean of AF (mm^2)	0.021	0.021	0.02
Density of AF (mm^2)	$1.31x10^2$	$1.23x10^2$	$1.32x10^2$

Table 2-2(b) Histomorphometric analysis data for IVD sham samples where values of all parameters reported as mean± SD (n=3)

HISTOLOGICAL ANALYSIS PARAMETERS	H&E STAIN (SHAM)	PR STAIN (SHAM)	AB STAIN (SHAM)
X(mm)	0.039	0.036	0.035
Z(mm)	0.037	0.034	0.034
Total AF in the ROI (mm^2)	1.69	1.59	1.78
Total proteoglycan in NP (mm)	-	-	0
Total proteoglycan in AF (mm)	-	-	1.48±0.2
Total collagen in NP (mm)	-	0	-
Total collagen in AF (mm)	-	1.62±0.3	-
Total new cell matrix in NP (mm)	0	-	-
Total new cell matrix in AF (mm)	1.48±0.3	-	-
Area of NP (mm^2)	1.61	1.71	1.67
Mean of NP (mm^2)	$3.15x10^{-3}$	$2.22x10^{-3}$	$4.72x10^{-3}$
Density of NP (mm^2)	$0.511x10^{3}$	$0.780x10^{3}$	$0.353x10^{3}$
Area of AF (mm^2)	3.38	3.28	3.3
Mean of AF (mm^2)	0.0198	0.018	0.021
Density of AF (mm^2)	$1.71x10^{2}$	$1.82x10^{2}$	$1.57x10^{2}$

Table 2-2(c) Histomorphometric analysis data for IVD pcl-pegda samples where values of all parameters reported as mean± SD (n=3)

HISTOLOGICAL ANALYSIS PARAMETERS	H&E STAIN (PCL-PEGDA)	PR STAIN (PCL-PEGDA)	AB STAIN (PCL-PEGDA)
X(mm)	0.035	0.035	0.036
Z(mm)	0.033	0.034	0.036
Total AF in the ROI (mm^2)	2.68	2.76	2.96
Total proteoglycan in NP (mm)	-	-	0.88±0.03
Total proteoglycan in AF (mm)	-	-	1.54±0.2
Total collagen in NP (mm)	-	0.86±0.03	-
Total collagen in AF (mm)	-	1.82±0.2	-
Total new cell matrix in NP (mm)	0.78±0.03	-	-
Total new cell matrix in AF (mm)	1.84±0.1	-	-
Area of NP (mm^2)	0.79	0.76	0.76
Mean of NP (mm^2)	$4.65x10^{-3}$	$5.5x10^{-3}$	$4.42x10^{-3}$
Density of NP (mm^2)	$0.216x10^3$	$0.138x10^3$	$0.175x10^3$
Area of AF (mm^2)	0.84	0.85	0.86
Mean of AF (mm^2)	0.018	0.019	0.016
Density of AF (mm^2)	$0.46x10^2$	$0.44x10^2$	$0.53x10^2$

Chapter 3

EFFECT OF BONE CEMENT AND TITANIUM IMPLANTS ON POLYCAPROLACTONE NANOFIBERS FOR TISSUE REGENERATION: AN *INVITRO* AND *INVIVO* STUDIES

3.1 SUMMARY

Most widely used implants in orthopedic and orthodontic surgeries such as titanium-based alloy is preferred because of their durability, mechanical and biological properties respectively. Cemented fixation of an implant, mainly used for osteoporotic bone, requires bone cement to hold in and around the implants due to the porosity of trabecular bone has been observed. The improvement of biomechanical performance of poly methyl methacrylate is seen accordingly and also, this study is based on the biocompatibility of a titanium rod implant that comes in contact with electro spun nanofibers made of PCL. [32, 33]Therefore, this study involves a titanium category of Ti-6AL-4V, modifying its aspect before implantation. Each case in this study incorporates various materials to observe the bone growth and its environment before moving towards surgery. This includes grooves on a titanium implant respectively as they are made and applied on the Ti rod using full spectrum laser, which is then treated with tesryl chloride for 48 hours followed by the application of fibernectin for 24 hours for the cell growth and implant to intensify. PCL nanofibers is later put into the rod with addition of collagen and implanted to the rabbit femur. Once the process of implantation is complete, the rabbit passes away, and 42 days later the rabbit femurs are collected. These samples are led to the sectioning process where live tissues are cut during its dehydration process with ethanol. Once dehydration is complete, technovit solution is used for polymerization and sectioning to begin and be taken for histomorphometric analysis respectively. [57]

3.2 INTRODUCTION

Bone is known to be a rigid body tissue that includes a combination of complex substances such as collagen and calcium phosphate. Its tissues provide protection of organs and other tissues and functions support during contraction and expansion of muscles, lungs respectively. According to Ti-6AL-4V, a titanium implant, is one the most used implants in the medical history because of its high strength, durability, biocompatibility, and other biological properties. For implantation to be successfully complete, biocompatibility of an implant and to attain good connection of the implants around the bone and surrounding tissue are necessary characteristics. Apart from its implant, bone cement is a certain material that is used in various orthopedic applications which provide a connection between the implant and cement.[25] We have recently developed an electro spun nanofiber membrane (ENFM) that can control the flow of cement into trabecular bone cavities using our patented electro spun nanofiber technology. To improve this efficiency and the relationship of the titanium implant, it is grooved with laser between each of them and PCL is applied followed by collagen. It is then treated with tesryl chloride for 48 hours along with fibernectin for 24 hours which helps the attachment and biocompatibility of cells on the surface. Finally, the implant is then coated with electro spun nanofibers between the grooves to enhance its cell growth and efficiency between the implants and bone cement surface.[58]

3.2.1 Fixation of Implants

Fixation of an implant using cement requires its bone cement to hold the implant in place. Therefore, it observes bone cement around the implant due to trabecular bone and its type respectively. Fractures located within the region tend to make the narrow confinement of tissue-cement interface. Localized fractures may occur at the tissue-cement interface by a relatively smaller force in compare to failure force of bone due to this heterogeneous flow of cement. [59] Electro spun nanofiber membrane (ENFM) is ready that can control the flow of cement into trabecular bone cavities using our patented electro spun nanofiber technology. This study has two objectives:

(1) to determine and improve the in vitro biocompatibility of the cement

(2) to determine whether the fixation of titanium implant improves the in vivo mechanical stability of the implant.

3.3 MATERIALS AND METHOD

This study involves materials such as titanium implants of Ti-6AL-4V, PCL pellets and acetone, an active reagent used in electrospinning of nanofibers. Apart from this, technovit 7200 VLC solution is used to join the materials together. Collagen is placed on the implant and is fixed to receive nanofibers which is then implanted in the femur of a rabbit. After 48 days of implantation, the rabbit passes away causing implants with the bone to be fixed in 10% formalin. Nanofibers are received through the sonicator machine followed by immediately pouring it into a syringe and attaching to a voltage power supply creating PCL fibers. Once fibers are obtained, histological analysis takes place which includes fixation, dehydration and polymerization respectively.

3.3.1 Preparation of samples

Rabbit cells were seeded at a density on cement samples and cultured for cell adhesion, proliferation, and differentiation assays in a custom made well. Ti wires were anchored in rabbit femur at the epiphyso–metaphyseal junction by three kinds of cement for in vivo studies (2nd objective): only PMMA, PMMA with titanium implant, PMMA with small to big groove. Animal studies were approved by OUHSC. Bilateral implantations were performed under anaesthetization on both legs. A 2.96 mm diameter and 6 mm deep hole was made by a hand drill in the rabbit femur. The ENFM cup was inserted into the hole

PMMA cement was prepared by hand mixing PMMA and titanium implants. The cement was injected into the hole of the ENFM cup by a syringe. Subsequently, each group of Ti wires was hand-pressed into the cement. The animal was euthanized after 8 weeks of implantation. The bone samples having Ti were cut using a diamond saw cutter. A custom-made fixture was used to permit coaxial alignment of Ti/bone sample.

3.3.1.1 Placement of cement surface

Bone cement is known to be a modern cementing technique that helps surface over a tissue while applying a respective implant to it. Here, Polymethyl methacrylate (PMMA) cement is applied to this tissue respectively. There are several stages into producing bone cement, its initial being mixing stage followed by addition of liquid to the powder and ends when the dough is homogenous and stirring become smoother. PMMA is known to dissolve in its monomer i.e. liquid wets the surface of the prepolymerized powder. Therefore, the prepolymerized beads expand and contact while some of them completely dissolve during mixing. At the end of mixing in Figure (4-1) , the cement becomes sticky and has consistency similar to toothpaste. This phase is followed by a waiting phase where it becomes sticky dough. It provides an indication of the level of adhesion.[60, 61] After this, working phase begins by knowing when the cement does not stick to the base anymore, but is of sufficiently low viscosity that even a doctor can use to apply the cement. Thus, its viscosity must be slowly monitored because with low viscosity, cement would not be able to withstand its bleeding pressure. Finally, the hardening or setting phase kicks in. This is the last phase in which polymerization stops and cement cures to a hard consistency. If implantation is completed with cement in the curing stage, it could result in the cement separating from the bone respectively.

3.3.2 Experimental analysis

3.3.2.1 Staining method

The rapid bone stain is preheated to approximately 55-60 °C by completely immersing the sample in a water bath or oven respectively. This is stained for a time duration of 30 seconds to 2 minutes in the rapid bone stain procedure. The stained sections in the sample are satisfied by adding acidified acid fuchsin for about 10-15 seconds. This is known as counterstain and is stained off, wiped by a laboratory wipe. Using this stain, it differentiates the picture well. In the picture, new cortical bone tends to have it stain to be dark pink while old cortical bone has light pink stain. Also, white color indicated that it has connective tissue between them while blue stain represents osteoid or cells within the marrow. The implants are categorized into a specific case: 42 days after

depending on the euthanization of a rabbit after implantation. The Figure shows the cell growth over a period.

3.4 HISTOMORPHOMETRIC ANALYSIS (HMA)

Bone histomorphometry is the quantitative analysis of bone micro architecture, quantification, and its function.[62] It usually provides information on bone turnover, remodelling and structure which cannot be obtained from other investigative approaches such as bone densitometry and biochemical markers. Current techniques are limited by the lack of reliable markers for activation and resorption. Therefore, quantification has been done and histology score is used to verify its images and to properly examine them once approved. According to figure, the titanium implants and cement are prepared before moving into surgery and 42 days later, the samples are collected and process of hard tissue on bone begins by putting them through dehydration and polymerisation to obtain solidified samples. This leads to staining, sectioning and images are captured accordingly to measure their parameters and the potential stability of bone cement and titanium implant in the rabbit femur.

3.4.1 Method of Analysis

3.4.1.1 Histological scoring

Bone injuries or defects have been an issue during analysis and therefore, tissue engineering have been enhanced to specific techniques. Histological assessment techniques are used beginning with its histological scoring system. This method is typically applied to quantitative and qualitative measurement in order to measure the amount present in the bone respectively. The histological sections were scored according to three key factors: Its bone maturity, cellular activity and cross-sectional area of the bone. It is scored from (0-4) where 0 is considered not present and 4 seems to be present and healthy to validate data from images.[63].

3.4.1.2 Bone J

Using BoneJ, a total new bone area is used to calculate the area of the connective tissue by determining the area of each tooth and combining them. This is converted into mm^2. Cortical bone area is measured by calculating the area of the cortical tissue present and converted into mm^2. New bone surface and cortical bone surface area are determined by quantifying its smoothness within its tissue. You may notice that there are small differences in its new bone surface. This is because of the amount of smoothness and large size of its tissue present. ROI (Region of interest) is calculated by finding its boundary within the bone tissue and disregarding the rest of the image. Tissue Volume is determined by finding its volume for the entire tissue in the image. This is converted into mm^3. Certain ratios are measured by calculating the total new bone and cortical bone to that of tissue volume.[60]

3.4.1.3 Problems faced during analysis

Problems may be related to measuring the bone tissue as there was cement involved while measuring because of its presence. Therefore, line is drawn wherever needed to evaluate accordingly and added along with the core measurement of bone analysis. Also, percent difference seemed to vary a little when comparing with other images however, each image depends on what type of material they have.

3.5 CONCLUSION

From the above results, we can conclude that the cell growth around the Titanium implant can be done by surface modifications of the implant and PCL nanofibers enhances the cell growth. According to the analyses, histomorphometry technique was able to signify each image with an implant and the comparison between them. Also, properties of samples of new cortical bone, old cortical bone and measurement of region of interest can be concluded from the present observation respectively. A percentage difference is calculated in order to compare it with previous established papers and their results to provide a perspective on each answer. Further studies can be done to determine the types of cells and its comparison using histomorphometric analysis around the implant.

This study advances orthopedic cement research by providing the understanding of how the biocompatibility and mechanical stability of cemented implants can be improved by surface modification of cement using nanoparticles and nanofibers. The novelty of this project is the in vitro and in vivo estimation of the cement-to- bone interface but can also be applied to anchor viscous (silicone) or granular (bone graft) materials with tissue.

3.6 FIGURES

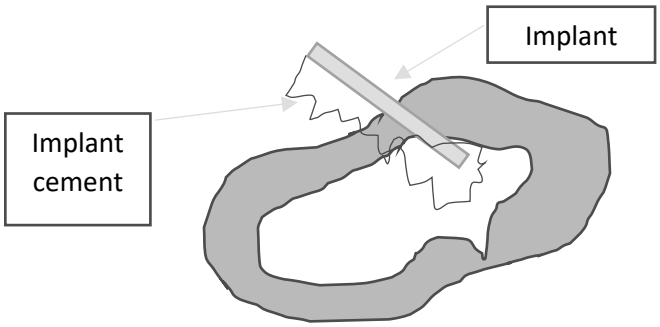

Figure 3-1 Schematic diagram of cement to implant system

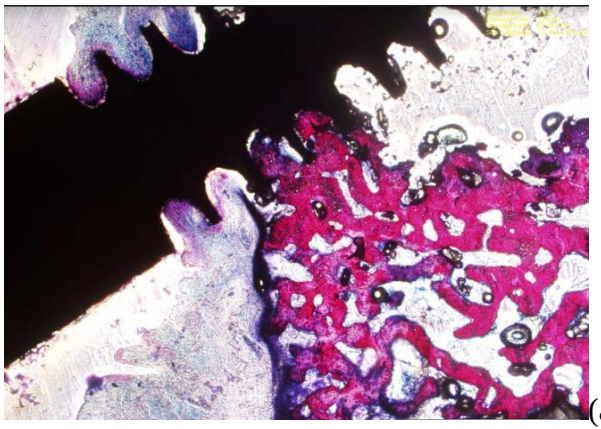

(a)

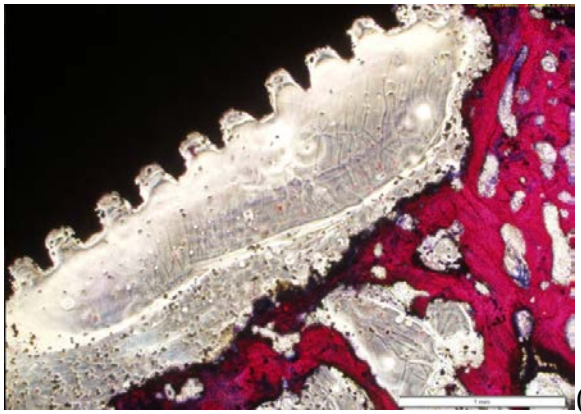

(b)

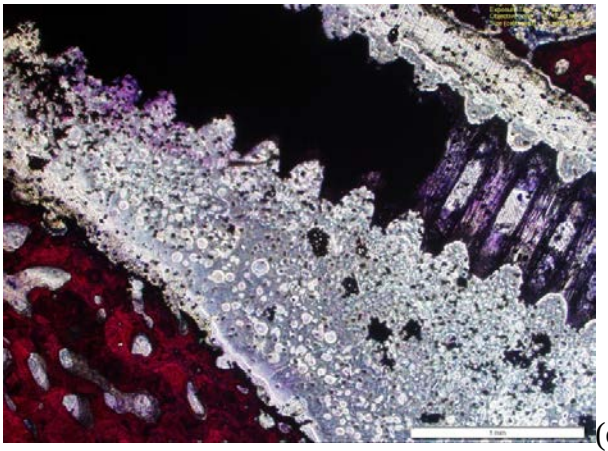

(c)

Figure 3-2 Cemented Samples (a) consisting of MgO sample (b) in contact with big groove, sample (c) with small groove

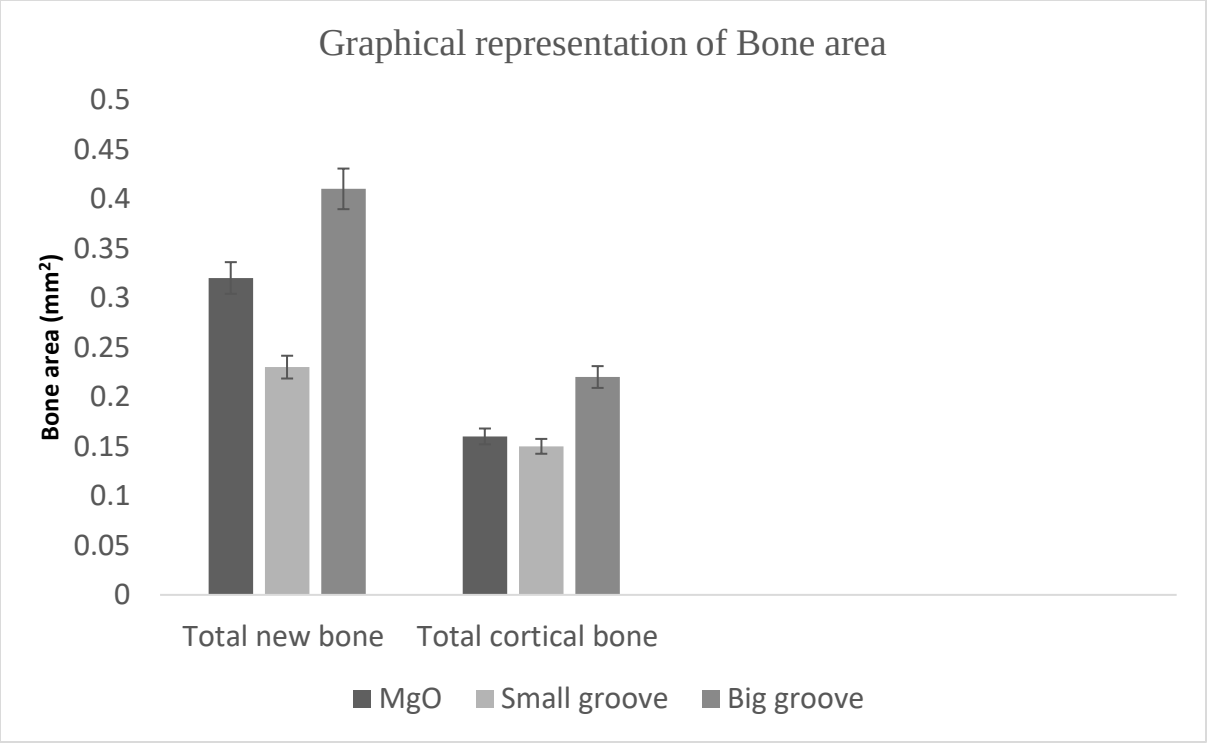

Figure 3-3(a) Plotted analysis of bone area in cemented samples for each sample

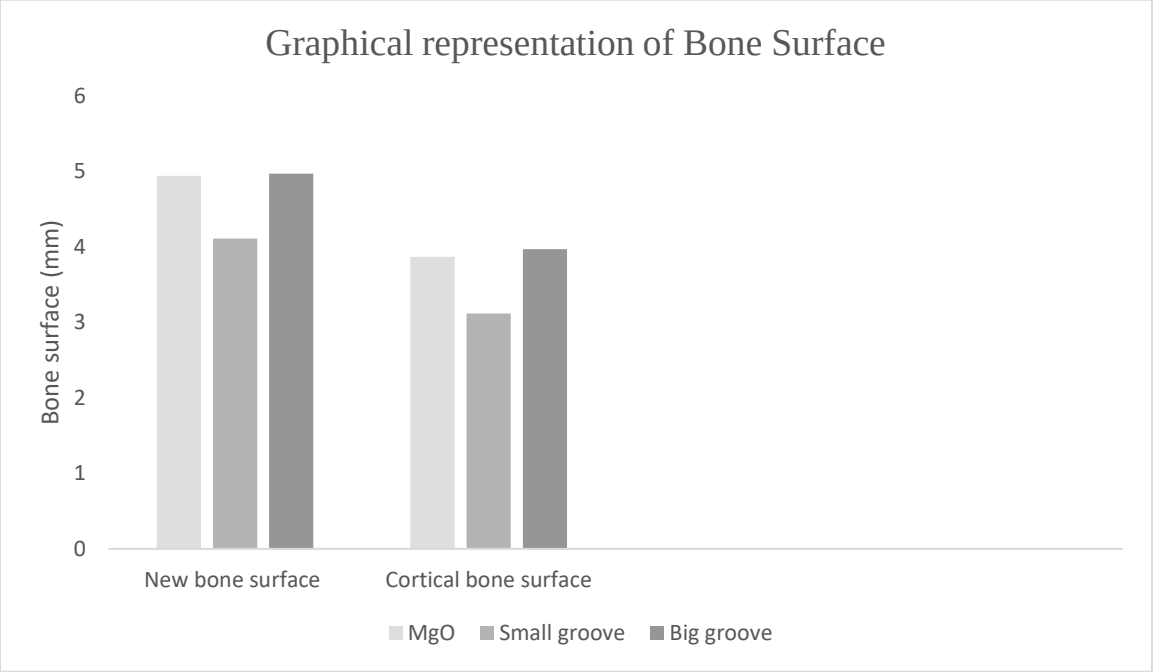

Figure 3-3 (b) Plotted analysis of bone surface in cemented samples for each sample

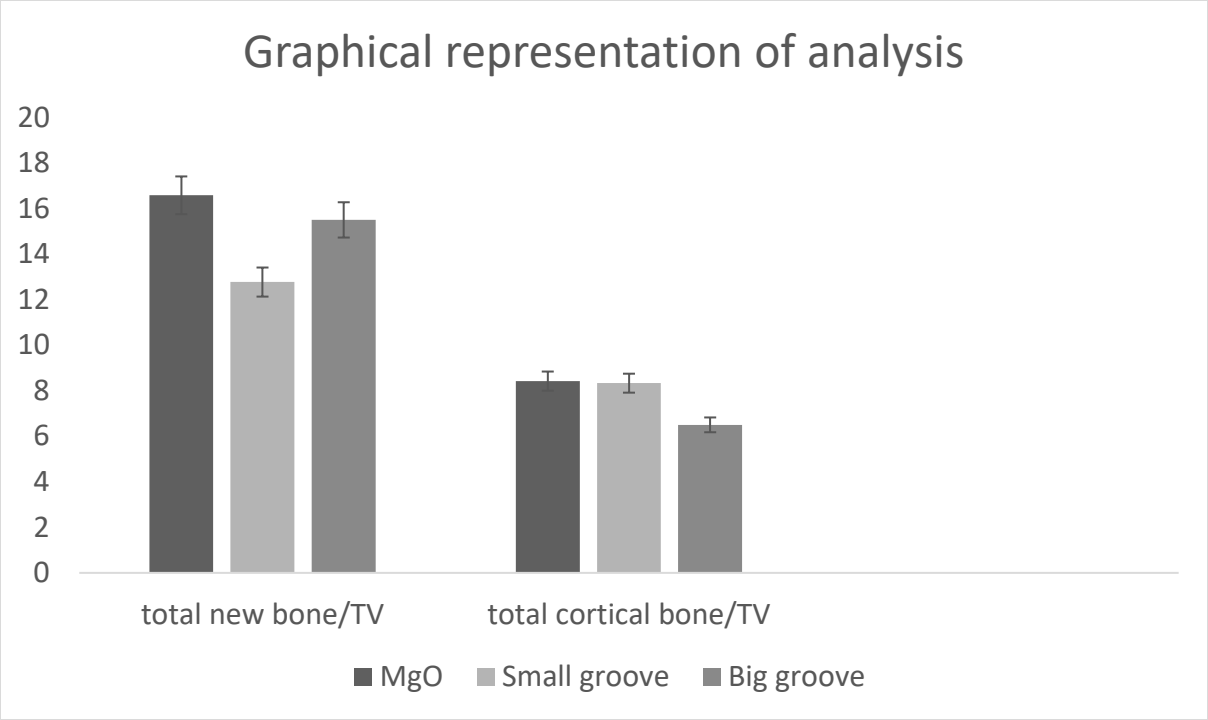

Figure 3-3(c)Continued plotted analysis of cemented samples for each sample

3.7 TABLES

Table 3-1 Histological scoring system regarding bone growth[63]

Cross-sectional area of bone	
No evidence of bone formation	
1-10% of implant shows evidence of bone formation	3
11-25% of implant shows evidence of bone formation	3
26-35% of implant shows evidence of bone formation	2
36-50% of implant shows evidence of bone formation	1
51-75% of implant shows evidence of bone formation	1
76-100% of implant shows evidence of bone formation	1
Bone maturity	
No bone	0
Immature/Unorganized	0
Immature	0
Mature	3
Mature/Well organized	3
Cellular activity	
None	0
Rare	1
Few	1
Moderate	4
Dense	3

Table 3-2 Analysis of samples present in (a)MgO, (b) in contact with big groove, (c) with small groove

	Images:	MgO	Small groove	Big groove
Parameters				
Total new bone area (mm2)		0.32	0.23	0.41
Total cortical bone area (mm2)		0.16	0.15	0.22
New bone surface (mm)		4.94	4.11	4.97
Cortical bone surface (mm)		3.87	3.12	3.97
ROI in the tissue area (mm)		1.71	3.36	3.21
Tissue Volume (TV)		0.019	0.018	0.02
total new bone/ TV (%)		16.8	12.77	15.5
total cortical bone/TV (%)		8.42	8.33	6.5
Bone to implant surface (mm)		8.46	6.42	7.25
Percent difference (%)		6.71	20.9	8.70

Table 3-3 Validation results from a referenced article [60]

Histological Analysis Parameters	Groove	Groove-NFM	
		Sample 1	Sample 2
Weight of animal before necropsy (kg)	2.55	2.62	2.65
Groove depth (μm) *	75.44 ± 0.28	88.10 ± 0.34	71.44 ± 0.11
% Bone to Implant Contact (%)	39.78	62.18	90.60
Total New Bone Area (mm^2)	0.02	0.36	0.29
Total Cortical Bone Area (mm^2)	0.00	0.15	0.26
Cortical Bone Surface (mm)	0.00	3.59	7.81
New Bone Surface (mm)	1.29	11.23	13.12
Total Tissue Area in the ROI (mm^2)	1.84	1.94	2.17
Total BV/TV (%)	1.01	26.18	25.63
Total New Bone/TV (%)	1.01	18.52	13.54
Total Cortical Bone/TV (%)	0.00	7.66	12.09

* There are 18 grooves per sample. Depth of all grooves were reported as mean ± SEM.

Chapter 4

EFFECT OF CHRACTERIZATION AND ANALYSIS OF THE EPIDERMIS IN SKIN

4.1 SUMMARY

The development of skin graft using rat dermal fibroblast cells is made through cell culture, electro spun nanofibers and histological sectioning. Cell culture is done briefly by thawing rat dermal fibroblast cells and aspirating the dish with various solutions such as trypsin and media. Once aspiration is complete, a significant process is done and placed in a hemocytometer. Cell count is conducted, and the solution is transferred into a test tube. Once transferred, centrifuge process takes place with a speed of 4.5 and time of 9 minutes. A 24-well is filled with a mix of solutions with specific ratios for each well to have equal distribution of solution. [64]Thus, nanofibers are later placed in each well and determines the growth and shape or the cells within the dish. The goal was to develop histomorphometric analysis protocol that can be used for skin equivalent model histomorphometric analysis. In general, skin tissue engineering associates with combining scaffolds, tissue cells and active molecules into a functional skin epidermis tissue. The production of skin graft was done and carried out through analysis using cell viability, differentiation, proliferation, histological sectioning and imaging of an OCT. [65]Also, histomorphometric analysis was complete using image processing techniques such as ImageJ, Bartlett's test and one-way ANOVA test.

4.2 BACKGROUND AND SPECIFICATION

4.2.1 Introduction

The skin is the largest organ in the body. It is one of the most important organs of the body, since it protects the body from physical damages due to assault. The skin also regulates homeostasis and performs sensory functions. [66] Damaged skin is a situation that results in the skin losing its ability to perform the normal functions that can lead to various complications such as loss of fluid or infections. Non-healing wounds present a significant and increasing problem in

the health care system. There is a limited understanding of the biological process involved in wound repair, maintenance of skin structure and integrity. A functional engineering scaffolds development is required to understand this biological process. The development of collagen graft using rat dermal fibroblast cells is made through cell culture, electrospinning nanofibers, staining and histological sectioning. Its main goal is to produce a collagen graft with evaluation of in vivo process using image processing consisting of histomorphometric analysis. [67]
The structure, function, area and tissue stability engage in a pivotal role in various analysis such as cell adhesion, viability, differentiation, proliferation and morphometry for regeneration of epidermis tissue.

4.2.2 Collagen as a scaffold material

Hydrogel scaffolds can be tuned to resemble dermal tissues mechanical and biological properties. Collagen is a protein made up of amino acids and the most common type in the extracellular matrix (ECM), providing strength to the matrix and attachment sites. CG is combined with fibroblasts so that the tissue becomes mature. Mechanical and biodegradable PCL properties of type I collagen creates a CG-PCL graft as a skin substitute and is compared with a CG graft using the standard in vivo tests models. Dr. Khandaker and Dr. Vaughan's research group conducted in vivo efficacy of CG-PCL skin graft [68, 69] using inbred Wistar rat species. My image analysis tools are used for the histomorphometric examination of tissue phenotyping to assess impact of a genotype on tissue and the distribution of satellite cells relative to their associated myocyte as well as their parameters regarding its size, shape and assessment of various regions using MATLAB, Fiji and ImageJ.

4.2.3 Harvesting cells and its analysis

A 3D Skin graft was initially produced through cell culture using Rat dermal fibroblast cells with Collagen, PEGDA and PCL due to its stable biocompatibility and several applications within the tissue engineering field. It is then pierced into 24x24 layers of electro spun nanofibers at the top and bottom of the sample respectively. Once pierced, the sample was harvested and observed each day to notice its growth by using optical coherence tomography. This apparatus is a certain imaging

technique that uses low-coherence light to capture 2 and 3 dimensional images from within the cell tissue. It is applied in medical imaging and industrial nondestructive testing (NDT). Therefore, this process had led up to 21 days and were processed as frozen sections for histology process. Biocompatibility of tissues are observed over time. Generally, Image processing is the analyzing and manipulating of images using a computer[1, 7]. Therefore, Histomorphometric analysis is done by measuring its area, thickness, Region of Interest, Amount of collagen and cell density using this technique. Each parameter is obtained by specifying a certain region of dermis and epidermis in its image to calculate accordingly. Once measured, it is converted into the unit required from various tools.

4.3 MATERIALS AND METHOD

4.3.1 Sample preparation

4.3.1.1 Polycaprolactone (PCL) used in electro spun nanofiber mesh

This study involved materials such as RDF, rat dermal fibroblast cells used in cell culture to develop an epidermis through sectioning and processing. PEGDA, a prepolymer solution is used in the formation of cross linked polymeric system in tissue engineering based applications and 0.5 grams of PCL pellets by mixing it with 5 ml of acetone solution and placing it onto the sonic ranger set machine creating the final solution. [70]This final solution is poured into a syringe pump with an infuse rate of 0.05 and fibers are produced using 9 kilovolts power supply. For cell culture, this study uses media solution by taking DMEM and ABAM antibiotics, 5 ml each and FBS solution. 25 ml of serum is placed in a filter along with 470 ml of DMEM solution. This is filtered and another beaker is used where FBS serum filled with DMEM to put in the vacuum tube applying pressure for liquid to lower down. The former beaker is officially produced to become 5% media harvest mainly used for cell culture. Plastic rings are used in the electrospinning of nanofibers punched with a diameter of outer ring as 7mm and inner ring as 5mm. Rings are created and placed under UV for an hour to make them sterile. Well- made fibers were collected using a wooden block with two parallel electrodes attached to it. As nanofibers are produced, 24 layers are created on one side as well as another 24 layers on the other creating a designated sandwich between the

hydrogels. This project develops a protocol to quantity tissue phonotype in collagen-polycaprolactone skin graft.

4.3.1.2 24 well-plate procedure

According to the sample preparation, rat dermal fibroblast cells are thawed out from -150 °C freezer and immediately sprayed with 70% ethanol. Once cells are warm enough, a dish with media and rdf cells is placed in a corner. Another dish is used to put fresh 5% harvest media along with rdf cells and mixed well. This is placed in the incubator for approximately 2 hours for cell culture to begin. Once the cell culture and electrospinning of nanofibers process is complete, a 24-well is taken out and rings are placed in each well respectively. 5 ml of trypsin is filled and distributed into each well and held for 5 mins for the cells to rise. Once risen, the cells must be able to move around freely within the dish and cells are counted accordingly. This solution is finally placed into a test tube in addition to 5 ml of media. From the test tube, 10 µl of this solution is set on a hemocytometer on both sides. Thus, these cells are counted and results in a specific measurement. This solution is put into a test tube and processed for centrifuge with a speed of 4.5m/s and a duration of 9 minutes. Once centrifuged, a white palette is seen at the bottom and therefore, solution is aspirated leaving the palette in the test tube. Each well is now placed with a mixture of 3.15 ml of water, 1.5 ml of CG, 1.45 ml premix and 0.5 ml of cell solution in accordance to the respective sequence. Rings must be held down in each well for approximately 15 minutes and placed in the incubator for 45 minutes.

4.3.2 Experimental Analysis

4.3.2.1. SEM Examination

To perceive embedded fibers in each group of hydrogels, each scaffold was viewed under Hitachi TM (Chiyoda, Tokyo, Japan) 3000 SEM. SEM image was captured on the flat surface of each scaffold. [71]To view the internal architecture of each scaffold, all samples were embedded in paraffin. The paraffin embedded samples were cut in longitudinal sections using a microtome. Multiple micro sections were produced and were captures as SEM images accordingly.

4.3.2.2 Degradation and OCT analysis

During each day, observation is made to make sure analysis and growth is observed accordingly. During the 7th day of harvesting, the 24-well plate consisting of epidermis cells are transferred to a 6-well plate with appropriate measurements. Nucleotides are taken out and placed in centrifuge for a few seconds. An addition of 3µl is poured into two new wells along with 1.5 ml of media. An Optical Coherence Tomography apparatus is used to take pictures of its development over a period. These pictures are collected and led to analysis. This procedure is similarly completed on the 14th and 21st day respectively. During the 28th day, 15% of sucrose present in the PBS solution is applied to the well plate and simultaneously, pictures from an OCT are obtained. The next day, which is the 29th day involves 30 % if sucrose in PBS solution with a certain measurement of 7.5-gram sucrose and 25 ml of PBS solution. Later, it is placed in a vortex and heated twice until specific crystals are dissolved. Liquid consisting of 15 % sucrose is discarded in the vials and replaced with 30 % of sucrose setting this overnight. On the 30th and final day, images are taken and moved into histological process.

4.3.2.3 Histological process (Frozen sectioning)

Cell solution is placed in paraffin wax with separate vials. With these vials, they are dipped into liquid nitrogen for a few seconds for the entire vial to become solid enough to section. Generally, paraffin blocks are known to be easy and smooth enough to section due to its consistency. These blocks are carried out by embedding to make sure the tissue is stable and represents a critical source of data. Thus, the vial is sectioned slowly and into thin slices using a cryostat machine. Once slices are obtained from various angles, each slice is placed on a microscopic slide and histologic process is done. These sections prepare display analysis involving morphology of the skin graft tissue, respectively.

Its procedure involves a sequence of steps: Each slide is set overnight at room temperature and the rest in jars. Once set, the slide is dipped into PBS solution for a duration of 15 minutes while simultaneously filtering hematoxylin. This slide is now positioned in hematoxylin for approximately 5 minutes. Later, it is positioned into distilled water until its clear. While cleared, the slide is left into 70 % ethyl alcohol for at least 3 minutes. Next, it is placed in eosin which is a

fluorescent dye derived from fluorescein and transferred into a solution of 70% ethyl alcohol for 5 minutes. Following by this step, 95 % ethyl alcohol is used by dipping the slide into it for 5 minutes twice. Similarly, 100 % ethyl alcohol is used twice for 5 minutes. Once this is complete, the slide is finally mixed into 100% xylene. The histologic slide is officially let to dry and mounted with permount (i.e.) an acrylic resin. This process is continued for all the sectioned microscopic slides in an interval of 5 minutes.

4.4 HISTOMORPHOMETRIC ANALYSIS (HMA)

Histomorphometry is the calculation based on the anatomy of a tissue. According to skin analysis, the samples were used for the following techniques: (a) Hematoxylin and eosin (H&E) staining for the morphological observation and morphometric analysis of the epidermis and dermis thickness, (b) Quantification including its region of interest, thickness and length of the image in which each image is compared with one or the other (c) Cell mapping of images to create a blended 3-dimensional image. These images were taken using an Olympus fluorescent microscope Bx41 with a magnification of 10 x respectively once embedded in paraffin followed by its staining procedure respectively.

4.4.1 Method of Analysis

The analysis begins with obtaining statistics of each sample. There is no specific number of statistics and once obtained, Bartlett's test is conducted. In this study, Bartlett's test is a certain procedure that assesses the assumption of loss. It is mainly used to face one's fear by analyzing a group of variances that are equal across groups of samples. Once found by using the test placed in excel sheet, a final value p is given to apply towards the quantification application. One-way ANOVA was used to analyze data analysis of skin thickness and collagen concentration data. It basically determines if there are any present values between various groups. The dermis and epidermis thickness in the same group was statistically compared using the Bartlett test, while the Bonferroni test was used for comparisons between the different types of skin. However, since the

skin images belong to the same group, Bonferroni test is not necessary. Once values from one-way ANOVA test is complete, it is placed into SPSS statistic software. Due to cost restrictions, the values were set aside in the SPSS software and found through image j and converted accordingly.

4.4.1.1 Bartlett's test

This test is used to calculate the homogeneity of variances and is associated with the one-way ANOVA test. In this test, a spreadsheet is made using Microsoft excel (made by the university of Delaware) and usually provides the value of 'p' for each variance of the image. By initially calculating its statistics comprising of its variances which undergo a hypothesis test that records the weight in grams. [72]The weights are placed in the excel sheet which helps calculate its pool variances along with value of 'q'. Test statistic is finally calculated with an outcome of 'p' value for each image and is used in the one-way ANOVA test.

4.4.1.2 one-way ANOVA test

It is an omnibus test that provides an overall effect causing differences between each group. This provides certain values in order to find the epidermis and dermis thickness as it is the core part of evaluation essential to be done. [9] Thus, data analysis is done through its plug in where each data from the image is received accordingly and plugged into the main test. This helps find its own 'p' value and is therefore, compared with the value received from Bartlett's test respectively. As $p \leq 0.5$, it must indicate that it is less than 5 % determining that null hypothesis is rejected and that a significant difference does exist.

4.4.1.3 Image J

This analysis helps find the area as well as region of interest (ROI) of an image. It also finds several other factors as well. Total skin thickness is measured by evaluating its entire skin and can use the help of bone j to determine thickness and can also be found by analyzing and setting scale with its

known distance. This can be applied to epidermis and dermis thickness by drawing its layer and calculating accordingly. Length and density are part of the ImageJ plug in which analyzes, sets measurements and converts to its units respectively.

4.4.1.4 Problems with analysis

Certain problems may arise due to variation in its measurements. This mainly happens when each image has artifacts due its compression ad therefore, it must either be in png or of tiff form to get values similar to each other. Another problem may occur where thickness may not be uniform everywhere and so it can be measured by finding thickness from each different location of the image and estimating its mean by averaging the measurements.

4.5 RESULTS AND DISCUSSION

There were no significant morphological differences among fragments of the same skin type. However, some differences between the epidermis and dermis thickness were observed. Thus, well-defined epidermis and dermis limits were observed in the samples. According to the table, they tend to be similar in measurement but slightly different from sample C respectively. This is because sample C has a larger epidermis and several hair follicles causing it to create a bigger value. Before obtaining these values, if the p- value is greater than 0.05, the one-way ANOVA test values must run a post hoc test which rules out warranting but must not be carried out. As for p-value being less than 0.05, before reporting results, one must follow up the test by running through the post-hoc test. Post hoc tests are known to identify the differences carried out in each tumble creating an overall difference in group means. [73]There are a great number of post-hoc tests that one can use but one can only be running as the official test. Turkey's HSD test is provided as one of the standard tests to use. The figure present in amalgamation is a certain image that creates a three-dimensional image from two dimensional in fact, for future work, analysis should be used for our skin equivalent model when the pictures are available.

4.5.1 Overlapping

Blending is the process of combining or uniting images together to create a certain three-dimensional image from two-dimensional images. The amalgamation of these images in Figure (4-6) help understands the type of skin one can see once after they analyze each sample. Since each sample belongs to the same category and is taken from each angle, it can conclude by providing a glimpse of actual skin from a rat respectively.

4.6 CONCLUSION

As a conclusion, the invitro and in vivo analysis of skin algorithm has been proved. Although there were some differences in the skin images, it managed to detect those abnormalities and analyze accordingly. P value of the images were less than 0.05 which turned out to be significantly different from each other. Therefore, this technique will be used for further analysis when the skin images from the in vivo preparation come through respectively.

4.7 FIGURES

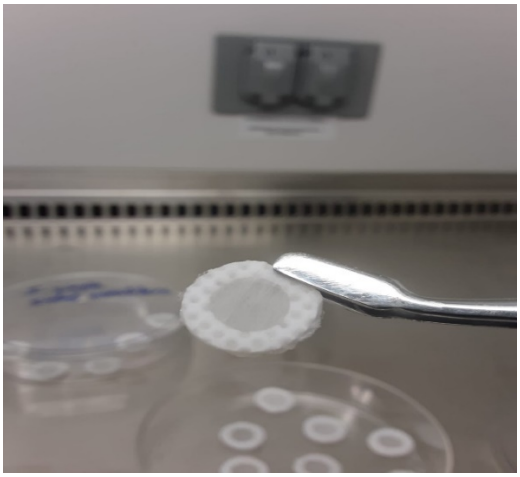

Figure 4-1 A PCL coated CG sample on a plastic ring

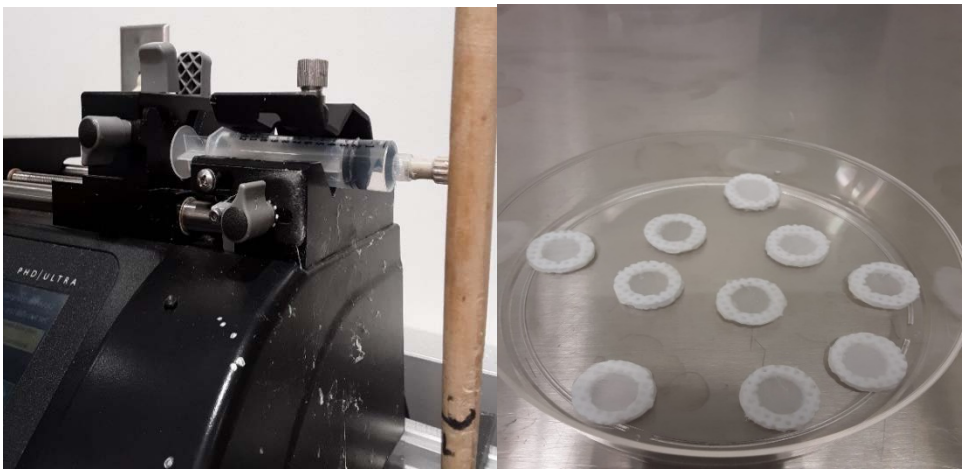

Figure 4-2 (a) Final solution is poured into a syringe pump to produce nanofibers (b) PCL coated nanofiber mesh around a ring

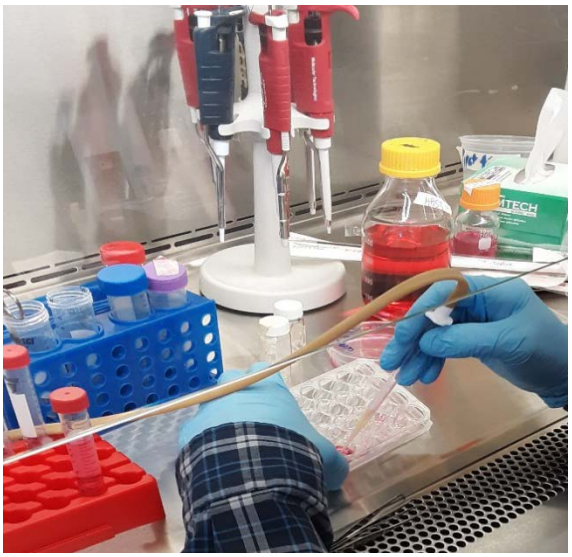

Figure 4-3 Cell solution being placed in each well-plate

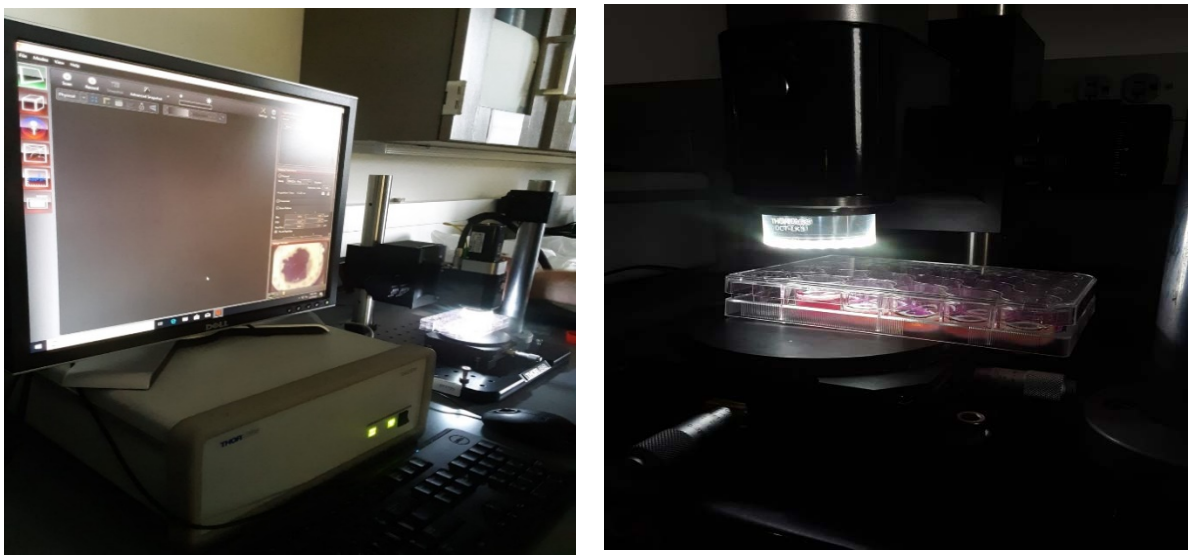

Figure 4-4 (a) Pictures being taken under an OCT (courtesy of Dr,Gang Xu) during the harvesting of cells, (b) Closer look of the well-plate being placed under a microscope associated with OCT imaging

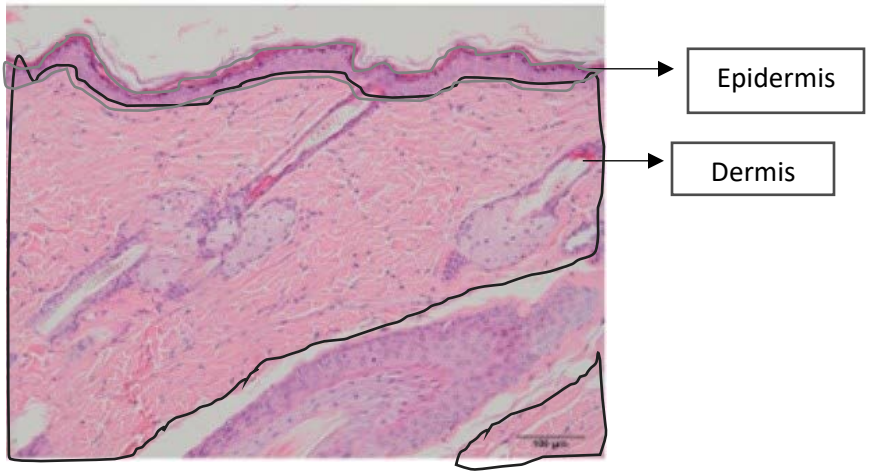

Figure 4-5 Identification of dermis and epidermis in an image[74]

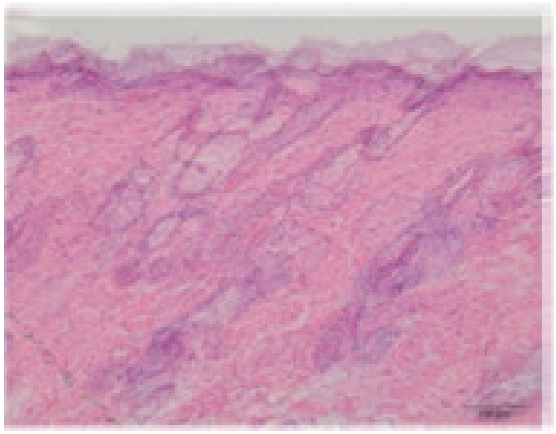

Figure 4-6 Blended image of the combination of the skin samples provided below to create a three-dimensional image[74]

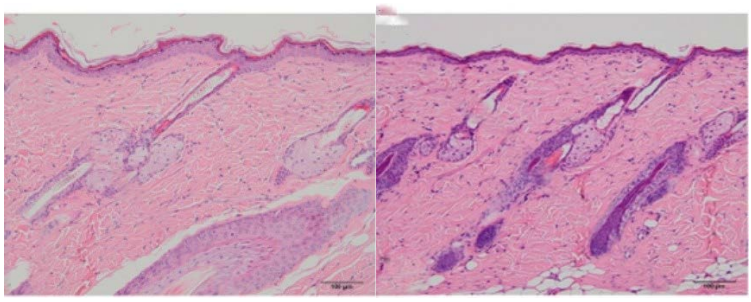

(a) (b)

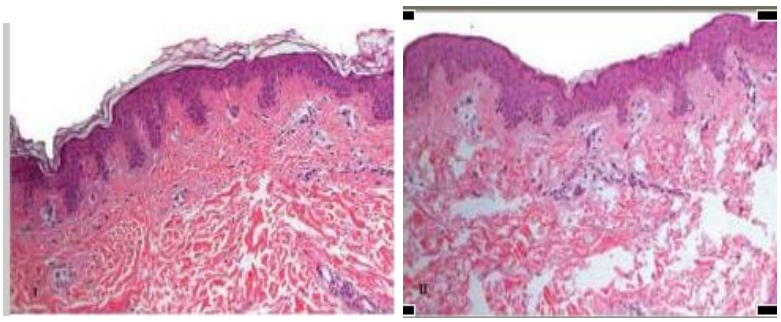

(c) (d)

Figure 4-7 Samples showing histopathology of skin in: (a) epithelium in healthy male rat [74], (b) epithelium in health female rat, (c)Epithelium in male epidermis, (d) Epithelium in female epidermis[75, 76]

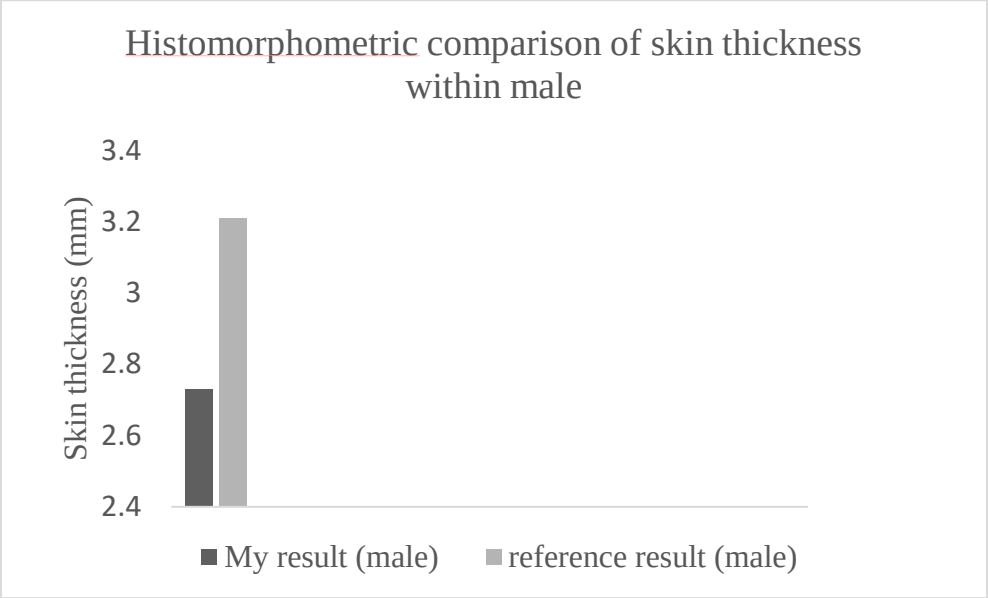

(a)

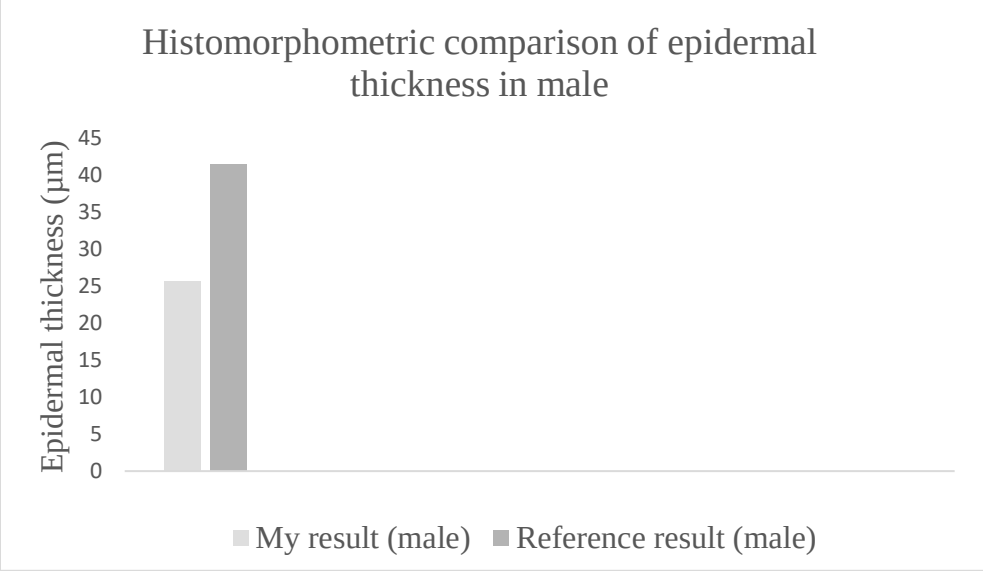

(b)

Figure 4-8 Histomorphometric comparison of (a) skin thickness and (b) epidermal thickness in male.

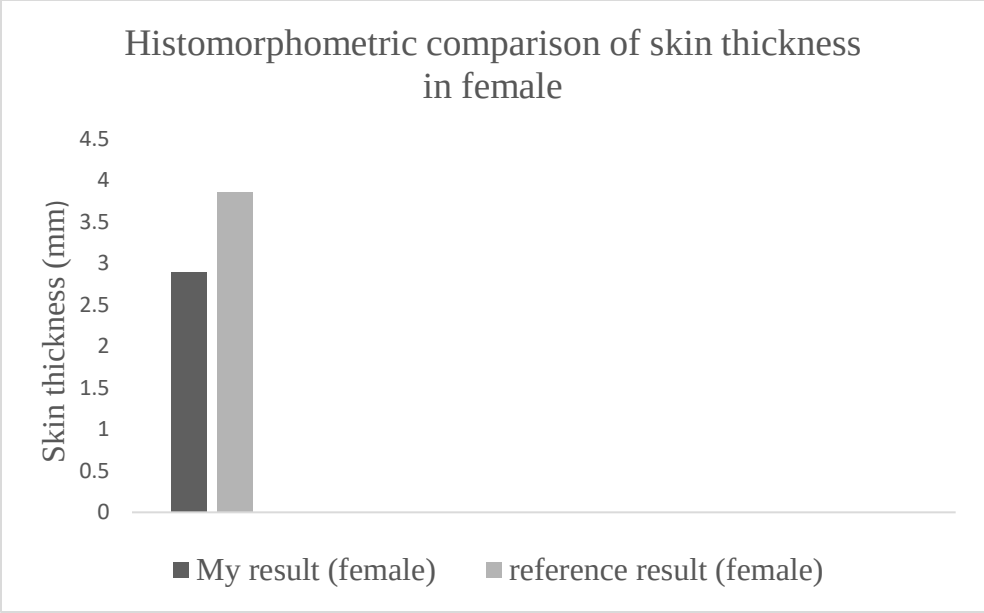

(a)

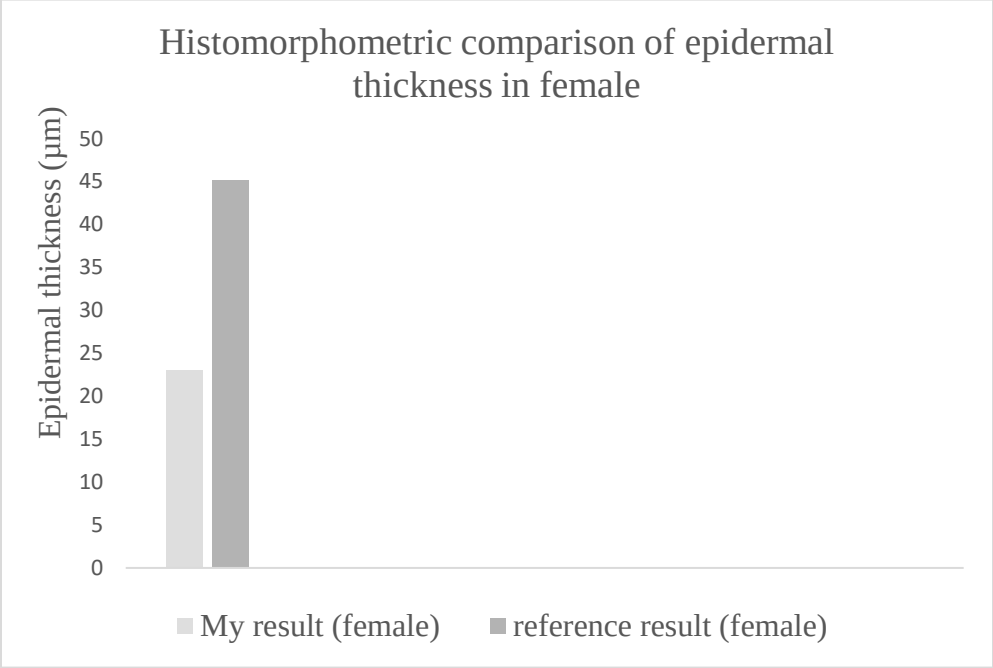

(b)

Figure 4-9 Histomorphometric comparison of (a) skin thickness and (b) epidermal thickness in female.

4.8 TABLES

Table 4-1 Analysis of skin in both (a) epithelium in healthy male rat, (b) epithelium in health female rat

		A	B
Total Skin thickness (mm)		2.49±0.24	2.59±0.31
Epidermis thickness (µm)		25.03±0.69	22.45±0.56
Dermis thickness (mm)		2.35±0.19	2.45±0.26
ROI (mm^2)		2.22	2.29
Epidermis Density (mm^2)		$0.32x10^3$	$0.38x10^3$
Dermis Density(mm^2)		$1.05x10^3$	$1.18x10^3$
Epidermis length(mm)		0.064	0.063
Dermis length(mm)		0.003	0.002

Table 4-2 Analysis of skin in both (c) acanthosis of male rats applied tape, (d) acanthosis of female rats applied tape

	C	D
Total Skin thickness (mm)	2.14±0.21	2.24±0.25
Epidermis thickness (μm)	31.12±0.74	26.22±0.54
Dermis thickness (mm)	2.02±0.17	2.15±0.21
ROI (mm^2)	3.02	2.14
Epidermis Density (mm^2)	$0.59x10^3$	$0.41x10^3$
Dermis Density(mm^2)	$1.77x10^3$	$1.24x10^3$
Epidermis length(mm)	0.011	0.002
Dermis length(mm)	0.006	0.002

Chapter 5

CONCLUSION AND FUTURE WORK

5.1 CONCLUSION

The goal of this research developed an algorithm and improved its biological functions of IVD samples and Titanium implants. This study used various techniques mainly electrospinning of nanofibers, cell culture, histological staining procedure and histomorphometric analysis. According to skin analysis, the study concluded that histomorphometric analysis delivered the evaluation and quantification of skin using RDF cells through Bartlett's test and Image J where a specific value (p) is found using the former test and applied to the one-way ANOVA test obtaining it's epidermis and dermis thickness respectively. With Image J, this tool helps in quantifying the number of cells present in its region by measuring its area, density and region of interest.

For Intervertebral disc, the structure and function are validated accordingly as the images taken under a fluorescent microscope are precise and clear. Biology analysis gave good results showing that cell viability was also present. Number of cells were viable, and differentiation was not as high as expected. According to its three samples, the values of NP and AF are similar between the native and pcl-pegda samples causing it to be stable enough to become a functioned implant.

The study involving titanium implant architecture is achieved by using bone histomorphometry providing information on its cellular activity respectively. The results can determine enough time necessary for PMMA cement to gain its functions followed by titanium implants. Using Bone J, quantification was done by calculating its analysis regarding the cortical bone. Certain differences are present between the cemented samples of bone followed by its area and volume due to its size and smoothness. The bone tissue analyses its region of boundary finding it to be its region of interest (ROI) along with its volume for the entire tissue. Its originality and analysis protocol can be held at continuous condition.

5.2 FUTURE WORK

Further histomorphometric analysis can now be done on the available Intervertebral disc, skin and cemented TI samples with this algorithm and concept. Using this preliminary study, skin samples can be further analyzed using the method of Bartlett's test and one-way ANOVA system and can further quantify various skin types from various cells. We know that PCL-PEGDA is an alternate implant when required within the Intervertebral disc and can be later used to further test certain tissues with its compatibility. It can become more biocompatible as its tensile strength can be further increased by adopting conventional nanofiber producing techniques like electrospinning. Furthermore, for analysis of bone, more parameters can be determined with various implants. Samples can be further processed to obtain the type of cell growth around the Titanium implant and bone cement. Also, the amount of bone to implant contact (BIC) followed by its volume can be calculated.

Chapter 6

6.1 REFERENCES

1. Milkulka, *ImageJ plug-ins for microscopic image processing.* 34th International Conference on Telecommunications and Signal Processing (TSP), 2011.
2. Nagel, *Image analysis and Mathematical Morphology. Volume 2: Theoretical Advances.* Journal of Microscopy, 1988. **2**: p. 597-597.
3. Varela, A. and J. Jolette, *Bone Toolbox: Biomarkers, Imaging Tools, Biomechanics, and Histomorphometry.* Toxicol Pathol, 2018. **46**(5): p. 511-529.
4. Goodarzi, N., et al., *Histomorphometrical and stereological study of the oesophagus in the adult male Persian squirrel (Sciurus anomalus).* Anat Histol Embryol, 2019. **48**(5): p. 444-448.
5. Erben, R.G. and M. Glosmann, *Histomorphometry in Rodents.* Methods Mol Biol, 2019. **1914**: p. 411-435.
6. Aragon-Sanchez, J., et al., *ImageJ: A Free, Easy, and Reliable Method to Measure Leg Ulcers Using Digital Pictures.* Int J Low Extrem Wounds, 2017. **16**(4): p. 269-273.
7. Wheeler, R.J., *ImageJ for Partially and Fully Automated Analysis of Trypanosome Micrographs.* Methods Mol Biol, 2020. **2116**: p. 385-408.
8. Schneider, C.A., W.S. Rasband, and K.W. Eliceiri, *NIH Image to ImageJ: 25 years of image analysis.* Nat Methods, 2012. **9**(7): p. 671-5.
9. ANOVA, O.-w. *one-way anova*. 2018; Available from: https://statistics.laerd.com/statistical-guides/one-way-anova-statistical-guide.php.
10. McHugh, M.L., *Multiple comparison analysis testing in ANOVA.* Biochem Med (Zagreb), 2011. **21**(3): p. 203-9.
11. Coakley, A., et al., *A comparison of imaging software and conventional cell counting in determining melanocyte density in photodamaged control sample and melanoma in situ biopsies.* J Cutan Pathol, 2020.
12. Doube, M., et al., *BoneJ: Free and extensible bone image analysis in ImageJ.* Bone, 2010. **47**(6): p. 1076-9.
13. Corrigan, A.M., et al., *IA-Lab: A MATLAB framework for efficient microscopy image analysis development, applied to quantifying intracellular transport of internalized peptide-drug conjugate.* PLoS One, 2019. **14**(8): p. e0220627.
14. Carney, K.R., et al., *LongAxis: A MATLAB-based program for 3D quantitative analysis of epithelial cell shape and orientation.* Dev Biol, 2020. **458**(1): p. 1-11.
15. Hodneland, E., et al., *CellSegm - a MATLAB toolbox for high-throughput 3D cell segmentation.* Source Code Biol Med, 2013. **8**(1): p. 16.
16. Butler, D.G.a.T., R. , *Tissue engineering and regenerative medicine.* Journal of Tissue Engineering and Regenerative Medicine

2012. **6**: p. 1-429.

17. Mertz, *Tissue engineering and Regenerative medicine: The promise, the challenges, the future*

IEEE Pulse, 2017. **8(3)**

p. 15-18.

18. Schenke-Layland, K. and H. Shin, *Call for Review Papers: Tissue Engineering, Part B.* Tissue Eng Part C Methods, 2020.
19. Schenke-Layland, K. and H. Shin, *Call for Review Papers: Tissue Engineering, Part B.* Tissue Eng Part B Rev, 2020.
20. Schenke-Layland, K. and H. Shin, *Call for Review Papers: Tissue Engineering, Part B.* Tissue Eng Part A, 2020.
21. Bowles, R.D. and L.A. Setton, *Biomaterials for intervertebral disc regeneration and repair.* Biomaterials, 2017. **129**: p. 54-67.
22. Piazza, N., et al., *Therapeutic Potential of Extracellular Vesicles in Degenerative Diseases of the Intervertebral Disc.* Front Bioeng Biotechnol, 2020. **8**: p. 311.
23. Sandor, Z., G.K. Rathonyi, and E. Dinya, *Assessment of Lumbar Lordosis Distribution with a Novel Mathematical Approach and Its Adaptation for Lumbar Intervertebral Disc Degeneration.* Comput Math Methods Med, 2020. **2020**: p. 7312125.
24. Oryan, A., S. Alidadi, and A. Moshiri, *Platelet-rich plasma for bone healing and regeneration.* Expert Opin Biol Ther, 2016. **16**(2): p. 213-32.
25. Dimitriou, R., et al., *Bone regeneration: current concepts and future directions.* BMC Med, 2011. **9**: p. 66.
26. Buser, Z., et al., *Synthetic bone graft versus autograft or allograft for spinal fusion: a systematic review.* J Neurosurg Spine, 2016. **25**(4): p. 509-516.
27. Vasrshney, *Polymethyl-methacrylate (PMMA, Plexigas, bone cement, acrylic Bone Cement).* Essential Orthopedics: Principles and Practice (2 Volumes), 2016: p. 1142-1142.
28. Caetano, G.F., et al., *Comparison of collagen content in skin wounds evaluated by biochemical assay and by computer-aided histomorphometric analysis.* Pharm Biol, 2016. **54**(11): p. 2555-2559.
29. Sidney rothbard, R.F.W., *Antigencity of rat collagen: Demonstration of antibody to rat collagen in the renal glomeruli of rat by fluorescence microscopy.* journal of experimental medicine, 1961. **113(6)**: p. 1041-1052.
30. Brianezi, G., et al., *Evaluation epidermal p53 immunostaining by digital image analysis.* Skin Res Technol, 2013. **19**(1): p. e108-12.
31. Bosworth, L.A., L.-A. Turner, and S.H. Cartmell, *State of the art composites comprising electrospun fibres coupled with hydrogels: a review.* Nanomedicine, 2013. **9**(3): p. 322-335.
32. Khandaker, M., et al., *Use of Polycaprolactone Electrospun Nanofibers as a Coating for Poly(methyl methacrylate) Bone Cement.* Nanomaterials (Basel), 2017. **7**(7).
33. Khandaker, M., et al., *Effect of Collagen-Polycaprolactone Nanofibers Matrix Coating on the In Vitro Cytocompatibility and In Vivo Bone Responses of Titanium.* Journal of Medical and Biological Engineering, 2018. **38**(2): p. 197-210.
34. Siddiqui, N., et al., *PCL-Based Composite Scaffold Matrices for Tissue Engineering Applications.* Mol Biotechnol, 2018. **60**(7): p. 506-532.
35. Grossen, P., et al., *PEG-PCL-based nanomedicines: A biodegradable drug delivery system and its application.* J Control Release, 2017. **260**: p. 46-60.
36. Guilak, B., F. P. , *Functional tissue Engineering: Ten more years of progress.*

. Journal of Biomechanics, 2014. **47(9)**: p. 1931-1932.
37. Teoh, S.H., B.T. Goh, and J. Lim, *Three-Dimensional Printed Polycaprolactone Scaffolds for Bone Regeneration Success and Future Perspective.* Tissue Eng Part A, 2019. **25**(13-14): p. 931-935.

38. Robo, C., et al., *In vivo response to a low-modulus PMMA bone cement in an ovine model.* Acta Biomater, 2018. **72**: p. 362-370.
39. Hwang, T.I., et al., *Fabrication of Bioabsorbable Polylactic-Co-Glycolic Acid/Polycaprolactone Nanofiber Coated Stent and Investigation of Biodegradability in Porcine Animal Model.* J Nanosci Nanotechnol, 2020. **20**(9): p. 5360-5364.
40. McGovern, J.A., M. Griffin, and D.W. Hutmacher, *Animal models for bone tissue engineering and modelling disease.* Dis Model Mech, 2018. **11**(4).
41. Thukkaram, M., et al., *Investigation of Ag/a-C:H nanocomposite coatings on titanium for orthopedic applications.* ACS Appl Mater Interfaces, 2020.
42. Bosshardt, D.D., V. Chappuis, and D. Buser, *Osseointegration of titanium, titanium alloy and zirconia dental implants: current knowledge and open questions.* Periodontol 2000, 2017. **73**(1): p. 22-40.
43. Kronenberg, D., et al., *Increased Collagen Turnover Impairs Tendon Microstructure and Stability in Integrin alpha2beta1-Deficient Mice.* Int J Mol Sci, 2020. **21**(8).
44. Sorushanova, A., et al., *The Collagen Suprafamily: From Biosynthesis to Advanced Biomaterial Development.* Adv Mater, 2019. **31**(1): p. e1801651.
45. Bowles, R.D., et al., *Tissue-engineered intervertebral discs produce new matrix, maintain disc height, and restore biomechanical function to the rodent spine.* Proceedings of the National Academy of Sciences, 2011. **108**(32): p. 13106-13111.
46. Browning, M.B. and E. Cosgriff-Hernandez, *Development of a biostable replacement for PEGDA hydrogels.* Biomacromolecules, 2012. **13**(3): p. 779-86.
47. Hong, J., et al., *Cell-Electrospinning and Its Application for Tissue Engineering.* Int J Mol Sci, 2019. **20**(24).
48. Chen, H., Y. Liu, and Q. Hu, *A novel bioactive membrane by cell electrospinning.* Exp Cell Res, 2015. **338**(2): p. 261-6.
49. Coleman, R., *Picrosirius red staining revisited.* Acta Histochem, 2011. **113**(3): p. 231-3.
50. Duffett, R.E., *Hematoxylin-neutral-red; a stain for cell inclusions and certain tissue elements.* Stain Technol, 1949. **24**(2): p. 73-7.
51. Stain, A.B., *alcian blue stain protocol.* IMVS Division of Pathology.
52. Wang, W., et al., *A label-free approach to detect cell viability/cytotoxicity based on intracellular xanthine/guanine by electrochemical method.* J Pharmacol Toxicol Methods, 2019. **100**: p. 106625.
53. staining, H.E., *Hematoxylin and Eosin (H&E) Staining Protocol.* IMVS Division of Pathology.
54. Chen, S., et al., *Meniscus, articular cartilage and nucleus pulposus: a comparative review of cartilage-like tissues in anatomy, development and function.* Cell Tissue Res, 2017. **370**(1): p. 53-70.
55. Holguin, N. and M.J. Silva, *In-Vivo Nucleus Pulposus-Specific Regulation of Adult Murine Intervertebral Disc Degeneration via Wnt/Beta-Catenin Signaling.* Sci Rep, 2018. **8**(1): p. 11191.
56. Wang, Y., et al., *Bioinformatics analysis reveals different gene expression patterns in the annulus fibrosis and nucleus pulpous during intervertebral disc degeneration.* Exp Ther Med, 2018. **16**(6): p. 5031-5040.
57. M.Khandaker, *Effect of polycaprolactone nanofiber coating on polyethylene glycol diacrylate scaffolds for tissue regeneration: An invitro and invivo studies.* 2020.
58. Dempster, D.W., et al., *Standardized nomenclature, symbols, and units for bone histomorphometry: a 2012 update of the report of the ASBMR Histomorphometry Nomenclature Committee.* J Bone Miner Res, 2013. **28**(1): p. 2-17.

59. Vidal, B., et al., *Bone histomorphometry revisited.* Acta Reumatol Port, 2012. **37**(4): p. 294-300.
60. Khandaker, M., et al., *Peen treatment on a titanium implant: effect of roughness, osteoblast cell functions, and bonding with bone cement.* Int J Nanomedicine, 2016. **11**: p. 585-94.
61. Wang, J., Q, *High-viscosity bone cement for vertebral compression fractures: A prospective study on intravertebral diffusion of bone cement.* Research square, 2020.
62. Vedi, S., & Compston, J, *Bone histomorphometry.* Bone research protocols 2003: p. 283-298.
63. Hamilton P.T, J.M., Ganesan S, Benson RE, Hyde-Deruyscher R, Beyer WF, Gile JC, Nair SA, Hodges JA, Grøn H., *Improved bone morphogenetic protein-2 retention in an injectable collagen matrix using bifunctional peptides.* PLoS Biol, 2013. **8(8)**.
64. Philippeos, C., et al., *Introduction to cell culture.* Methods Mol Biol, 2012. **806**: p. 1-13.
65. Gabriele, M.L., et al., *Optical coherence tomography: history, current status, and laboratory work.* Invest Ophthalmol Vis Sci, 2011. **52**(5): p. 2425-36.
66. Boudana, D., et al., *[History of skin graft].* Ann Chir Plast Esthet, 2010. **55**(4): p. 328-32.
67. Rosin, N.L., et al., *Collagen structural alterations contribute to stiffening of tissue after split-thickness skin grafting.* Wound Repair Regen, 2016. **24**(2): p. 263-74.
68. Pasquali-Ronchetti I, B.-C.M., *Elastic fiber during development and aging.* Microsc Res Tech

1997. **38(4)**: p. 428-435.
69. Eltom, Z., G., & Muhammad, A. , *Scaffold techniques and designs in tissue engineering functions and purposes: A review.*

. Advances in Materials Science and Engineering, 2019: p. 1-13.
70. da Fonseca, G.F., et al., *Scaffolds of PCL combined to bioglass: synthesis, characterization and biological performance.* J Mater Sci Mater Med, 2020. **31**(5): p. 41.
71. Nowell, J.A. and J.B. Pawley, *Preparation of experimental animal tissue for SEM.* Scan Electron Microsc, 1980(Pt 2): p. 1-19.
72. test, B., *https://www.itl.nist.gov/div898/handbook/eda/section3/eda357.htm*.
73. Khanna, R., A. Chandra, and R.K. Singh, *Quantitative evaluation of masking effect of resin infiltration on developmental defects of enamel.* Quintessence Int, 2020: p. 2-9.
74. Mitsuishi, M., et al., *Histological dermal changes caused by preparation and application procedures in percutaneous dose toxicity studies in dogs, rabbits and rats.* J Toxicol Pathol, 2015. **28**(1): p. 1-9.
75. Inforzato, H.C.B., et al., *Histomorphometric analysis of the skin of women during the reproductive period.* Clinics (Sao Paulo), 2018. **73**: p. e387.
76. Wei, J.C.J., et al., *Allometric scaling of skin thickness, elasticity, viscoelasticity to mass for micro-medical device translation: from mice, rats, rabbits, pigs to humans.* Sci Rep, 2017. **7**(1): p. 15885.